

Linear and Weakly Non-Linear Stability Analyses of Double-Diffusive Electro-Convection in a Micropolar Fluid

S. Pranesh¹ and Sameena Tarannum²

¹Department of Mathematics, Christ University, Bangalore, India.

²Department of Professional Studies, Christ University, Bangalore, India.

Abstract: The linear and weakly non-linear stability analyses of double diffusive electro-convection in a micropolar fluid layer heated and saluted from below and cooled from above is studied. The linear and non-linear analyses are, respectively based on normal mode technique and truncated representation of Fourier series. The influence of various parameters on the onset of convection has been analyzed in the linear case. The resulting autonomous Lorenz model obtained in non-linear analysis is solved numerically to quantify the heat and mass transfers through Nusselt and Sherwood number. It is observed that the increase in concentration of suspended particles and electric field and electric Rayleigh number increases the heat and mass transfer.

Keywords: Double diffusive convection, Micropolar fluid, Electro-convection, autonomous Lorenz model and Nusselt and Sherwood number.

I. Introduction

The instability in a fluid due to two opposing density altering components with differing molecular diffusivity, like temperature and salt or any two solute concentrations is called double diffusive convection. The differences between single and double diffusive system is that in double diffusive system convection can occur even when the system is hydrostatically stable if the diffusivities of the two diffusing fields are different.

The study of double diffusive convection gained a tremendous interest in the recent years due to its numerous fundamental and industrial applications. Oceanography is the root of double-diffusive convection in natural settings. The existence of heat and salt concentrations at different gradients and the fact that they diffuse at different rates lead to spectacular double-diffusive instabilities known as “salt-fingers” (Stern 1960). The formation of salt-fingers can also be observed in laboratory settings. Double-diffusive convection occurs in the sun where temperature and Helium diffusions take place at different rates. Convection in magma chambers and sea-wind formations are among other manifestations of double-diffusive convection in nature. The theory of double diffusive convection both theoretically and experimentally was investigated by (Turner 1973; Jin and Chen et al. 1997; Malashetty et al. 2006; Pranesh and Arun 2012) and more recently by Bhadauria and Pal 2014).

Double diffusive convection encountered in many practical problems involves different types of dissolved substances of chemical that are freely suspended in the fluid and they will be executing microrotation forming micropolar fluid. The presence of these suspended particles plays a major role in mixing processes. Although double diffusive convection in Newtonian fluid has been studied extensively, the problem considering the above facts has not received due attention in the literature. When the particles are freely suspended there will be translational and rotational motion relative to fluid. One way of tackling this is to follow the elegant and rigorous model proposed by Eringen called “micropolar fluid model”.

The model of micropolar fluids (Eringen 1964) deals with a class of fluids, which exhibits certain microscopic effects arising from the local structure and micro-motions of the fluid elements. These fluids can support stress moments and body moments and are influenced by the spin inertia. Consequently new principles must be added to the basic principle of continuous media which deals with conservation of micro inertia moments and balance of first stress moments. The theory of micro fluids naturally gives rise to the concepts of inertial spin, body moments, micro-stress averages and stress moments which have no counterpart in the classical fluid theories. A detailed survey of the theory of micropolar fluid and its applications are considered in the books of (Eringen 1966; Eringen 1972; Lukaszewicz 1999; Power 1995). The theory of thermomicropolar convection was studied by many authors (Datta and Sastry 1976; Ahmadi 1976; Rao 1980; Lebon and Gracia 1981; Bhattacharya and Jena 1983; Siddheshwar and Pranesh 1998; Pranesh and Riya 2012) and recently by (Joseph et al. 2013; Pranesh et al. 2014).

Thus the objective of this paper is to study the effect of suspended particles and electric field on the onset of double diffusive convection using linear theory and also its effects on heat and mass transfer using weakly non-linear analysis. With these objectives we now move on to the formulation of the problem.

II. Mathematical Formulation Of The Problem

Consider a horizontal layer of infinite extent occupied by a Boussinesquian, micropolar fluid of depth ‘d’ as shown in figure (1). Let ΔT and ΔC be the difference in temperature and species concentration of the fluid between lower and upper plates and uniform ac electric field is applied in the vertical direction. For Mathematical tractability we confine ourselves to two dimensional rolls so that all physical quantities are independent of y coordinate. Further, the boundaries are assumed to be free, perfect conductors of heat, permeable, spin vanishing boundary conditions and tangential component of electric field is continuous. Appropriate single-phase heat and solute transport equations are chosen with effective heat capacity ratio and effective thermal diffusivity.

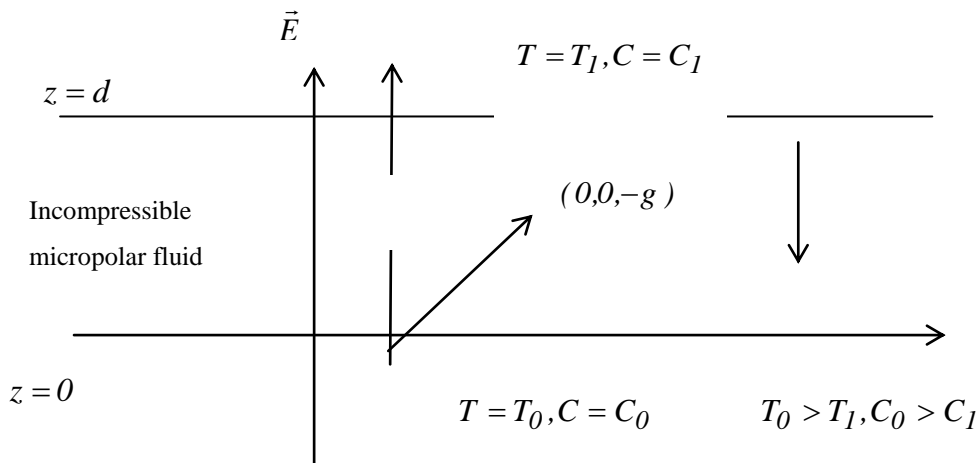


Figure 1: Schematic diagram for the problem

The governing equations for the double diffusive convection in a Boussinesquianmicropolar fluid are:

Continuity equation:

$$\nabla \cdot \vec{q} = 0, \tag{1}$$

Conservation of linear momentum:

$$\rho_0 \left[\frac{\partial \vec{q}}{\partial t} + (\vec{q} \cdot \nabla) \vec{q} \right] = -\nabla p - \rho \vec{g} \hat{k} + (2\zeta + \eta) \nabla^2 \vec{q} + \zeta \nabla \times \vec{\omega} + (\vec{P} \cdot \nabla) \vec{E}, \tag{2}$$

Conservation of angular momentum:

$$\rho_0 I \left[\frac{\partial \vec{\omega}}{\partial t} + (\vec{q} \cdot \nabla) \vec{\omega} \right] = (\lambda' + \eta') \nabla (\nabla \cdot \vec{\omega}) + \eta' \nabla^2 \vec{\omega} + \zeta (\nabla \times \vec{q} - 2\vec{\omega}), \tag{3}$$

Conservation of energy:

$$\frac{\partial T}{\partial t} + (\vec{q} \cdot \nabla) T = \frac{\beta}{\rho C_v} (\nabla \times \vec{\omega}) \cdot \nabla T + \chi \nabla^2 T, \tag{4}$$

Conservation of solute concentration:

$$\frac{\partial C}{\partial t} + (\vec{q} \cdot \nabla) C = \chi_s \nabla^2 C, \tag{5}$$

Equation of state:

$$\rho = \rho_0 [1 - \alpha_t (T - T_0) + \alpha_s (C - C_0)], \tag{6}$$

where, \vec{q} is the velocity, ρ_0 is density of the fluid at temperature $T = T_0$, p is the pressure, ρ is the density, \vec{g} is acceleration due to gravity, ζ is coupling viscosity coefficient or vortex viscosity, \vec{P} is dielectric polarization, \vec{E} is the electric field, λ and η are the bulk and shear spin-viscosity coefficients, $\vec{\omega}$ is the angular velocity, I is moment of inertia, λ' and η' are bulk and shear spin-viscosity coefficients, T is the temperature, C is the concentration, β is micropolar heat conduction coefficient, α_t is coefficient of thermal expansion, determining how fast the density decreases with temperature, α_s is coefficient of concentration expansion, determining how fast the density decreases with concentration, χ is the thermal diffusivity and χ_s is the solute diffusivity. $\chi_s \ll \chi$ implies that a particle in a configuration will dissipate heat quickly compared to concentration.

Since the fluid is assumed to be a poor conductor, the electric field may be considered as irrotational. Thus the electrodynamic equations are:

Faraday's law:

$$\nabla \times \vec{E} = 0, \vec{E} = -\nabla \phi \} \tag{7}$$

Equation of polarisation field:

$$\nabla \cdot (\epsilon_0 \vec{E} + \vec{P}) = 0, \vec{P} = \epsilon_0 (\epsilon_r - 1) \vec{E} \} \tag{8}$$

where, ϵ_r is the dielectric constant, ϵ_0 is the electric permittivity of free space and ϕ is the electric scalar potential.

The dielectric constant is assumed to be a linear function of temperature according to

$$\epsilon_r = \epsilon_r^0 - e(T - T_0) \tag{9}$$

where, $e > 0$ is the dielectric permittivity and $\epsilon_r^0 = 1 + \chi_e$ is electric susceptibility.

III. Basic State

The basic state of the fluid is assumed to be being quiescent and is described by:

$$\left. \begin{aligned} \vec{q}_b &= (0,0,0), \vec{\omega}_b = (0,0,0), p = p_b(z), \rho = \rho_b(z), \vec{E} = \vec{E}_b(z), \\ \vec{P} &= \vec{P}_b(z), T = T_b(z), \epsilon_r = \epsilon_{rb}(z), C = C_b(z), \end{aligned} \right\} \tag{10}$$

where, the subscript 'b' denotes the basic state.

The temperature T_b , pressure p_b , density ρ_b , polarization P_b and electric field E_b satisfy

$$\left. \begin{aligned} \frac{\partial^2 T_b}{\partial z^2} &= 0, \\ -\frac{\partial p_b}{\partial z} - \rho_0 g + P_b \frac{\partial E_b}{\partial z} &= 0, \\ \rho_b &= \rho_0 [1 - \alpha(T_b - T_0)], \\ \vec{E}_b &= \left[\frac{(1 + \chi_e) E_0}{(1 + \chi_e) + \frac{e \Delta T}{d} z} \right] \hat{k}, \\ \vec{P}_b &= \epsilon_0 E_0 (1 + \chi_e) \left[1 - \frac{1}{(1 + \chi_e) + \frac{e \Delta T z}{d}} \right] \hat{k}, \end{aligned} \right\} \tag{11}$$

where, E_0 is the root mean square value of the electric field at the lower surface.

IV. Stability Analysis

Let the basic state be disturbed by an infinitesimal thermal perturbation, we now have,

$$\left. \begin{aligned} \vec{q} &= \vec{q}_b + \vec{q}', \vec{\omega} = \vec{\omega}_b + \vec{\omega}', p = p_b + p', \rho = \rho_b + \rho', \\ \epsilon_r &= \epsilon_{rb} + \epsilon_r', \vec{E} = \vec{E}_b + (E_1' \hat{i} + E_3' \hat{k}), \vec{P} = \vec{P}_b + (P_1' \hat{i} + P_3' \hat{k}), \\ T &= T_b + T', C = C_b + C', \end{aligned} \right\} \tag{12}$$

where, the primes indicate that the quantities are infinitesimal perturbations and subscript 'b' indicates basic state value.

The second equation of (10) gives,

$$\left. \begin{aligned} P_1' &= \varepsilon_0 \chi_e E_1' - e \varepsilon_0 T' E_1' \\ P_3' &= \varepsilon_0 \chi_e E_3' - e \varepsilon_0 T' E_0' - e \varepsilon_0 T' E_3' \end{aligned} \right\}, \tag{13}$$

Substituting equation (12) into equations (1) to (9) and using the basic state solution, we get:

$$\nabla \cdot \vec{q}' = 0, \tag{14}$$

$$\rho_o \left[\frac{\partial \vec{q}'}{\partial t} + (\vec{q}' \cdot \nabla) \vec{q}' \right] = -\nabla p' - \rho' g \hat{k} + (2\zeta + \eta) \nabla^2 \vec{q}' + (\zeta \nabla \times \vec{\omega}') + \left. \begin{aligned} &+ (\vec{P}_b \cdot \nabla) \vec{E}' + (\vec{P}' \cdot \nabla) \vec{E}_b + (\vec{P}' \cdot \nabla) \vec{E}' \end{aligned} \right\}, \tag{15}$$

$$\rho_o I \left[\frac{\partial \vec{\omega}'}{\partial t} + (\vec{q}' \cdot \nabla) \vec{\omega}' \right] = (\lambda' + \eta') \nabla (\nabla \cdot \vec{\omega}') + (\eta' \nabla^2 \vec{\omega}') + \left. \begin{aligned} &+ \zeta (\nabla \times \vec{q}' - 2\vec{\omega}') \end{aligned} \right\}, \tag{16}$$

$$\frac{\partial T'}{\partial t} + (\vec{q}' \cdot \nabla) T' - w \frac{\Delta T}{d} = \chi \nabla^2 T' + \frac{\beta}{\rho_o C_r} \left[\nabla \times \vec{\omega}' \cdot \left(-\frac{\Delta T}{d} \right) \hat{k} \right] + \frac{\beta}{\rho_o C_r} \left[\nabla \times \vec{\omega}' \cdot \Delta T \right], \tag{17}$$

$$\frac{\partial C}{\partial t} + (\vec{q}' \cdot \nabla) C' - w \frac{\Delta C}{d} = \chi_s \nabla^2 C', \tag{18}$$

$$\rho = -\rho_o \alpha_t T' + \rho_o \alpha_s g C'. \tag{19}$$

Substituting equation (19) in equation (15), differentiating x-component of the equation with respect to z, differentiating z-component of the equation with respect to x and subtracting one resulting equation from the other, we get,

$$\rho_o \left[\frac{\partial \vec{q}'}{\partial t} + (\vec{q}' \cdot \nabla) \vec{q}' \right] = -\nabla p' + \rho_o \alpha_t T' g \hat{k} - \rho_o \alpha_s C' g \hat{k} + (2\zeta + \eta) \nabla^2 \vec{q}' + \left. \begin{aligned} &+ (\zeta \nabla \times \vec{\omega}') + (\vec{P}_b \cdot \nabla) \vec{E}' + (\vec{P}' \cdot \nabla) \vec{E}_b + (\vec{P}' \cdot \nabla) \vec{E}' \end{aligned} \right\}. \tag{20}$$

Writing y-component of equation (16), we get,

$$\rho_o I \frac{\partial \omega_y}{\partial t} + \left(u' \frac{\partial}{\partial x} + w' \frac{\partial}{\partial z} \right) \omega_y = \eta' \nabla^2 \omega_y + \zeta \left(\frac{\partial u'}{\partial z} - \frac{\partial w'}{\partial x} - 2\omega_y \right). \tag{21}$$

We consider only two dimensional disturbances and thus restrict ourselves to the xz-plane; we now introduce the stream functions in the form:

$$u' = \frac{\partial \psi'}{\partial z}, w' = -\frac{\partial \psi'}{\partial x}, \tag{22}$$

which satisfies the continuity equation (14).

On using equations (22) in equations (17), (18), (20) and (21), we get,

$$\rho_0 \frac{\partial}{\partial t} \left(\nabla^2 \psi \right) = -\alpha_t \rho_0 g \frac{\partial T}{\partial x} + \alpha_s \rho_0 g \frac{\partial C}{\partial x} + (2\zeta + \eta) \nabla^4 \psi - \zeta \nabla^2 \omega_y + \rho_0 J(\psi, \nabla^2 \psi) \quad (23)$$

$$\rho_0 I \frac{\partial \omega_y}{\partial t} = \eta' \nabla^2 \omega_y + \zeta (\nabla^2 \psi - 2\omega_y) + I \rho_0 J(\psi, \omega_y), \quad (24)$$

$$\frac{\partial T}{\partial t} = -\frac{\Delta T}{d} \frac{\partial \psi}{\partial x} + \chi \nabla^2 T - \left(\frac{\beta \Delta T}{\rho_0 C_r d} \right) \frac{\partial \omega_y}{\partial x} + \left(\frac{\beta}{\rho_0 C_r} \right) J(\omega_y, T) + J(\psi, T), \quad (25)$$

$$\frac{\partial C}{\partial t} = -\frac{\Delta C}{d} \frac{\partial \psi}{\partial x} + \chi_s \nabla^2 C + J(\psi, C), \quad (26)$$

where, J stands for Jacobian.

The equations (23)-(26) are non dimensionalized using the following definition:

$$\left. \begin{aligned} (x^*, y^*, z^*) &= \left(\frac{x'}{d}, \frac{y'}{d}, \frac{z'}{d} \right), t^* = \frac{t'}{d^2/\chi}, \psi^* = \frac{\psi'}{\chi/d}, T^* = \frac{T'}{\Delta T}, \\ C^* &= \frac{C'}{\Delta C}, \phi^* = \frac{\phi'}{eE_0 \Delta T d / (1 + \chi_e)}, \omega_z = \frac{(\nabla \times \vec{\omega})}{\chi/d^3}. \end{aligned} \right\} \quad (27)$$

Using equation (27) into equations (23)-(26) we get the dimensionless equations in the form (after neglecting the asterisks):

$$\left. \begin{aligned} \frac{1}{\text{Pr}} \frac{\partial}{\partial t} \left(\nabla^2 \psi \right) &= -R \frac{\partial T}{\partial t} + R_s \frac{\partial C}{\partial x} + (1 + N_1) \nabla^4 \psi - N_1 \nabla^2 \omega_y \\ &+ \frac{1}{\text{Pr}} J(\psi, \nabla^2 \psi) + L \frac{\partial^2 \phi}{\partial x \partial y} - L \frac{\partial T}{\partial t} + LJ \left(T, \frac{\partial \phi}{\partial z} \right) \end{aligned} \right\} \quad (28)$$

$$\frac{N_2}{\text{Pr}} \frac{\partial \omega_y}{\partial t} = N_3 \nabla^2 \omega_y + N_1 \nabla^2 \psi - 2N_1 \omega_y + \frac{N_2}{\text{Pr}} J(\psi, \omega_y), \quad (29)$$

$$\frac{\partial T}{\partial t} = -\frac{\partial \psi}{\partial x} + \nabla^2 T - N_5 \frac{\partial \omega_y}{\partial x} + N_5 J(\omega_y, T) + J(\psi, T), \quad (30)$$

$$\frac{\partial C}{\partial t} = -\frac{\partial \psi}{\partial x} + \Gamma \nabla^2 C + J(\psi, C), \quad (31)$$

$$\nabla^2 \phi = \frac{\partial T}{\partial z}. \quad (32)$$

The non-dimensional parameters Pr, R, R_s, N₁, N₂, N₃, N₅, L and Γ are as follows:

$$\text{Pr} = \frac{\mu}{\rho_0 \chi} \quad (\text{Prandtl number}),$$

$$R = \frac{\rho_0 \alpha g \Delta T d^3}{\chi(\zeta + \eta)} \quad (\text{Rayleigh number}),$$

$$R_s = \frac{\rho_0 \alpha_s g \Delta C d^3}{\chi(\zeta + \eta)} \quad (\text{Solutal Rayleigh number}),$$

$$N_1 = \frac{\zeta}{\zeta + \eta} \quad (\text{Coupling parameter}),$$

$$N_2 = \frac{I}{d^2} \quad (\text{Inertia parameter}),$$

$$N_3 = \frac{\eta'}{(\zeta + \eta)d^2} \quad (\text{Couple stress parameter}),$$

$$N_5 = \frac{\beta}{\rho_0 C_v d^2} \quad (\text{Micropolar heat conduction parameter}),$$

$$L = \frac{\epsilon_0 e^2 E_0^2 \Delta T^2 d^2}{(1 + \chi_e)(\zeta + \eta)\chi} \quad (\text{Electric Rayleigh number}),$$

$$\Gamma = \frac{\chi_s}{\chi} \quad (\text{Ratio of diffusivity}).$$

Equations (28)-(32) are solved for free-free, isothermal, permeable, zero electric potential and no-spin boundaries and hence we have,

$$\psi = \frac{\partial^2 \psi}{\partial z^2} = T = C = \omega_y = \frac{\partial \phi}{\partial z} = 0 \text{ at } z = 0, 1. \quad (33)$$

V. Linear Stability Theory

In this section, we discuss the linear stability analysis considering marginal state. The solution of this analysis is of great utility in the local non-linear stability analysis discussed in the next section. To make this study we neglect the Jacobians in equations (28)-(32). The linearized version of equations (28)-(32) are:

$$\left. \begin{aligned} \left[\frac{1}{\text{Pr}} \frac{\partial}{\partial t} - (1 + N_1) \nabla^2 \right] \nabla^2 \psi &= -(R + L) \frac{\partial T}{\partial t} + R_s \frac{\partial C}{\partial x} \\ &- N_1 \nabla^2 \omega_y + L \frac{\partial^2 \phi}{\partial x \partial y} \end{aligned} \right\} \quad (34)$$

$$\left[\frac{N_2}{\text{Pr}} \frac{\partial}{\partial t} + 2N_1 - N_3 \nabla^2 \right] \omega_y = N_1 \nabla^2 \psi, \quad (35)$$

$$\left[\frac{\partial}{\partial t} - \nabla^2 \right] T = -\frac{\partial \psi}{\partial x} - N_5 \frac{\partial \omega_y}{\partial x}, \tag{36}$$

$$\left[\frac{\partial}{\partial t} - \Gamma \nabla^2 \right] C = -\frac{\partial \psi}{\partial x}, \tag{37}$$

$$\nabla^2 \phi = \frac{\partial T}{\partial z}. \tag{38}$$

We assume the solution of equation (34) to (38) to be periodic waves (Chandrasekhar 1961) of the form:

$$\left. \begin{aligned} \psi &= \psi_0 \sin(\pi \alpha x) \sin(\pi z) \\ \omega_y &= \Omega_0 \sin(\pi \alpha x) \sin(\pi z) \\ T &= T_0 \cos(\pi \alpha x) \sin(\pi z) \\ C &= C_0 \cos(\pi \alpha x) \sin(\pi z) \\ \phi &= \frac{1}{\pi} \phi_0 \cos(\pi \alpha x) \cos(\pi z) \end{aligned} \right\}, \tag{39}$$

Substituting equation (39) into equations (34)-(38), we get,

$$\begin{bmatrix} -k^2 \left(\frac{\sigma}{\text{Pr}} + (1+N_1)k^2 \right) & -N_1 k^2 & -(R+L)\pi\alpha & R_s \pi\alpha & 0 \\ N_1 k^2 & \frac{\sigma}{\text{Pr}} N_2 + N_3 k^2 + 2N_1 & 0 & 0 & 0 \\ \pi\alpha & N_5 \pi\alpha & \sigma + k^2 & 0 & 0 \\ \pi\alpha & 0 & 0 & \sigma + \Gamma k^2 & 0 \\ 0 & 0 & -\pi & 0 & -\pi(1+\alpha^2) \end{bmatrix} \begin{bmatrix} \psi_0 \\ \Omega_0 \\ T_0 \\ C_0 \\ \phi_0 \end{bmatrix} = \begin{bmatrix} 0 \\ 0 \\ 0 \\ 0 \\ 0 \end{bmatrix} \tag{40}$$

where $k^2 = \pi^2(\alpha^2 + 1)$.

For a non-trivial solution of the homogeneous system (40) for $\psi_0, \Omega_0, T_0, C_0$ and ϕ_0 the determinant of the coefficient matrix must vanish. This leads on simplification to

$$R = \frac{(\sigma + \Gamma k^2)(\sigma + k^2)k^4 [X_1 X_2 - N_1^2 k^2] + R_s k^2 \pi^2 \alpha^2 (\sigma + k^2) X_1 + L \pi^2 \alpha^2 (\sigma + \Gamma k^2) (X_1 - N_1 N_5 k^2) (\pi^2 - k^2)}{\pi^2 \alpha^2 k^2 (\sigma + \Gamma k^2) (X_1 - N_1 N_5 k^2)}, \tag{41}$$

where,

$$X_1 = \frac{N_2 \sigma}{\text{Pr}} + N_3 k^2 + 2N_1,$$

$$X_2 = \frac{1}{\text{Pr}} \sigma + (1 + N_1) k^2.$$

5.1 Marginal State

For marginal stability convection σ in equation (41) must be real and the corresponding Rayleigh number R for marginal state is obtained by putting $\sigma = 0$ in equation (41) in the form:

$$R = \frac{\left[\Gamma k^8 (N_3(1 + N_1)k^4 + N_1(2 + N_1)k^2) + R_s k^4 \pi^2 \alpha^2 (N_3 k^2 + 2N_1) \right] + L \pi^2 \alpha^2 k^2 \Gamma (N_3 k^2 + 2N_1 - N_1 N_5 k^2) (\pi^2 - k^2)}{\pi^2 \alpha^2 k^4 \Gamma (N_3 k^2 + 2N_1 - N_1 N_5 k^2)}, \tag{42}$$

If $R_s = 0, L = 0$ and setting $\pi^2 \alpha^2$ as a^2 , equation (42) reduces to,

$$R = \frac{k^6 \left[N_3(1 + N_1)k^2 + N_1(2 + N_1) \right]}{a^2 \left[(N_3 - N_1 N_5)k^2 + 2N_1 \right]}, \tag{43}$$

which is the expression for the Rayleigh number discussed by (Datta and Sastry 1976; Bhattacharya and Jena 1983; Siddheshwar and Pranesh 1998) in the absence of magnetic field.

Setting $N_1 = 0$ and keeping N_3 and N_5 arbitrary in equation (43), we get,

$$R = \frac{k^6}{a^2}, \tag{44}$$

the classical Rayleigh – Benard result.

Repeating the same on equation (42), we get,

$$R = \frac{\Gamma k^6 + R_s a^2}{a^2 \Gamma}, \tag{45}$$

which is the expression for the Rayleigh number discussed by (Turner 1973).

VI. Finite Amplitude Convection

The finite amplitude analysis is carried out here via Fourier series representation of stream function ψ , the spin ω_y , the temperature distribution T , the concentration distribution C and electric potential ϕ . Although the linear stability analysis is sufficient for obtaining the stability condition of the motionless solution and the corresponding eigen functions describing qualitatively the convective flow, it cannot provide information about the values of the convection amplitudes, nor regarding the rate of heat and mass transfer. To obtain this additional information, we perform nonlinear analysis, which is useful to understand the physical mechanism with minimum amount of mathematical analysis and is a step forward towards understanding the complete nonlinear problem.

The first effect of non-linearity is to distort the temperature and concentration fields through the interactions of ψ and T, ω_y and C . The distortion of the temperature and concentration fields will correspond to a change in the horizontal mean, i.e., a component of the form $\sin(2\pi z)$ will be generated. Thus, truncated system which describes the finite-amplitude convection is given by (Veronis 1959):

$$\psi(x, y, t) = A(t) \sin(\pi\alpha x) \sin(\pi z), \tag{46}$$

$$\omega_y(x, y, t) = B(t) \sin(\pi\alpha x) \sin(\pi z), \tag{47}$$

$$T(x, y, t) = E(t) \cos(\pi\alpha x) \sin(\pi z) + F(t) \sin(2\pi z), \tag{48}$$

$$C(x, y, t) = G(t) \cos(\pi\alpha x) \sin(\pi z) + H(t) \sin(2\pi z), \tag{49}$$

$$\phi(x, z, t) = \frac{1}{\pi} M(t) \cos(\pi\alpha x) \cos(\pi z), \tag{50}$$

where, the time dependent amplitudes A, B, E, F, G, H and M are to be determined from the dynamics of the system. The functions ψ and ω_y do not contain an x-independent term because the spontaneous generation of large scale flow has been discounted.

Substituting equations (46) - (50) in to equations (28) - (32) and equating the coefficient of like terms we obtain the following non-linear autonomous system (Sixth order Lorenz model) of differential equations:

$$\left. \begin{aligned} \dot{A} = & \frac{-(R+L)\text{Pr}\pi\alpha}{k^2} E + \frac{R_s\pi\alpha\text{Pr}}{k^2} G - \text{Pr}(1+N_1)k^2 A - N_1\text{Pr}B \\ & + \frac{L\pi^3\alpha\text{Pr}}{k^4} E + \frac{4L\pi^6\alpha^3\text{Pr}}{k^4} EF \end{aligned} \right\} \tag{51}$$

$$\dot{B} = \frac{-N_3\text{Pr}k^2}{N_2} B - \frac{N_1\text{Pr}k^2}{N_2} A - \frac{2N_1\text{Pr}}{N_2} B, \tag{52}$$

$$\dot{E} = -\pi\alpha A - k^2 E - N_5\pi\alpha B - \pi^2\alpha A F - N_5\pi^2\alpha B F, \tag{53}$$

$$\dot{F} = -4\pi^2 F + \frac{1}{2} N_5\pi^2\alpha B E + \frac{1}{2} \pi^2\alpha A E, \tag{54}$$

$$\dot{G} = -\pi\alpha A - \Gamma k^2 G - \pi^2\alpha A H, \tag{55}$$

$$\dot{H} = -4\Gamma\pi^2 H + \frac{1}{2} \pi^2\alpha A G. \tag{56}$$

where, over dot denotes time derivative.

M in equation (50) is eliminated by substituting equations (48) and (50) in equation (32).

The generalized Lorenz model (51)-(56) is uniformly bounded in time and possesses many properties of the full problem. This set of non-linear ordinary differential equations possesses an important symmetry for it is invariant under the transformation,

$$(A, B, E, F, G, H) \rightarrow (-A, -B, -E, -F, -G, -H), \tag{57}$$

Also the phase-space volume contracts at a uniform rate given by:

$$\frac{\partial \dot{A}}{\partial A} + \frac{\partial \dot{B}}{\partial B} + \frac{\partial \dot{E}}{\partial E} + \frac{\partial \dot{F}}{\partial F} + \frac{\partial \dot{G}}{\partial G} + \frac{\partial \dot{H}}{\partial H} = - \left[\frac{\text{Pr}(1+N_1)k^2 + \frac{N_3\text{Pr}k^2}{N_2}}{+ \frac{2N_1\text{Pr}}{N_2} + (1+\Gamma)(k^2 + 4\pi^2)} \right], \tag{58}$$

which is always negative and therefore the system is bounded and dissipative. As a result, the trajectories are attracted to a set of measure zero in the phase space; in particular they may be attracted to a fixed point, a limit cycle or perhaps, a strange attractor.

VII. Heat And Mass Transport At Lower Boundary

Heat and mass transport in a double diffusive system depends on the imposed temperature and concentration differences on the diffusion coefficient. In this chapter we mainly focus on the influence of double diffusion on heat and

mass transport which are quantified in terms of Nusselt number (Nu) and Sherwood number (Sh). The heat transport can be quantified by a Nusselt number Nu and is defined as,

$$Nu = \frac{\text{Heat transport by (conduction + convection)}}{\text{Heat transport by (conduction)}},$$

$$Nu = \frac{\left[\frac{k}{2\pi} \int_0^{2\pi/k} (1 - z + T)_z dx \right]_{z=0}}{\left[\frac{k}{2\pi} \int_0^{2\pi/k} (1 - z)_z dx \right]_{z=0}}, \quad (59)$$

where subscript in the integrand denotes the derivative with respect to z.

Substituting equation (48) into equation (59) and completing the differentiation and integration, we get the following expression for Nusselt number:

$$Nu = 1 - 2\pi F(t). \quad (60)$$

The mass transport is quantified by Sherwood number Sh and is defined as

$$Sh = \frac{\text{Convection mass transfer coefficient}}{\text{Diffusive mass transfer coefficient}},$$

$$Sh = \frac{\left[\frac{k}{2\pi} \int_0^{2\pi/k} (1 - z + C)_z dx \right]_{z=0}}{\left[\frac{k}{2\pi} \int_0^{2\pi/k} (1 - z)_z dx \right]_{z=0}}, \quad (61)$$

where subscript in the integrand denotes the derivative with respect to z.

Substituting equation (49) into equation (61) and completing the differentiation and integration, we get the following expression for Sherwood number:

$$Sh = 1 - 2\pi H(t). \quad (62)$$

The amplitudes $F(t)$ and $H(t)$ are determined from the dynamics of the Lorenz system (51)-(56) which can be obtained by solving the system numerically.

VIII. Results And Discussions

Before embarking on the discussion of the results, we make some comments on the parameters that arise in the problem, which are $N_1, N_2, N_3, N_5, Pr, R_s, \Gamma, L$ and these influence the convective heat and mass transports. The first four refer the micropolar fluid parameters arise due to the micropolar fluid, next three arise due to the fluid and last one due to electric field. The range of values of micropolar fluid parameters are $0 \leq N_1 \leq 1, 0 \leq N_2 \leq r, 0 \leq N_3 \leq m$ and $0 \leq N_5 \leq n$, where the quantities r, m and n are finite positive real numbers. The range of values of N_1, N_2, N_3 and N_5 specified above is guided by the Clausius-Duhem inequality. A discussion on these is presented in (Siddheshwar and Pranesh 1998). The values of Pr for fluid with suspended particles are considered to be greater than those for a liquid without suspended particles

because of presence of suspended particles increases the viscosity. Positive values of R_s are considered, and these signify the assumption of a situation in which we have cool fresh water overlying warm salty water.

$$1 \quad L = 50, \Gamma = 0.1, N_3 = 2, N_5 = 1, R_s = 25$$

$$2 \quad L = 100, \Gamma = 0.1, N_3 = 2, N_5 = 1, R_s = 25$$

$$3 \quad L = 200, \Gamma = 0.1, N_3 = 2, N_5 = 1, R_s = 25$$

$$4 \quad L = 100, \Gamma = 0.3, N_3 = 2, N_5 = 1, R_s = 25$$

$$5 \quad L = 100, \Gamma = 0.5, N_3 = 2, N_5 = 1, R_s = 25$$

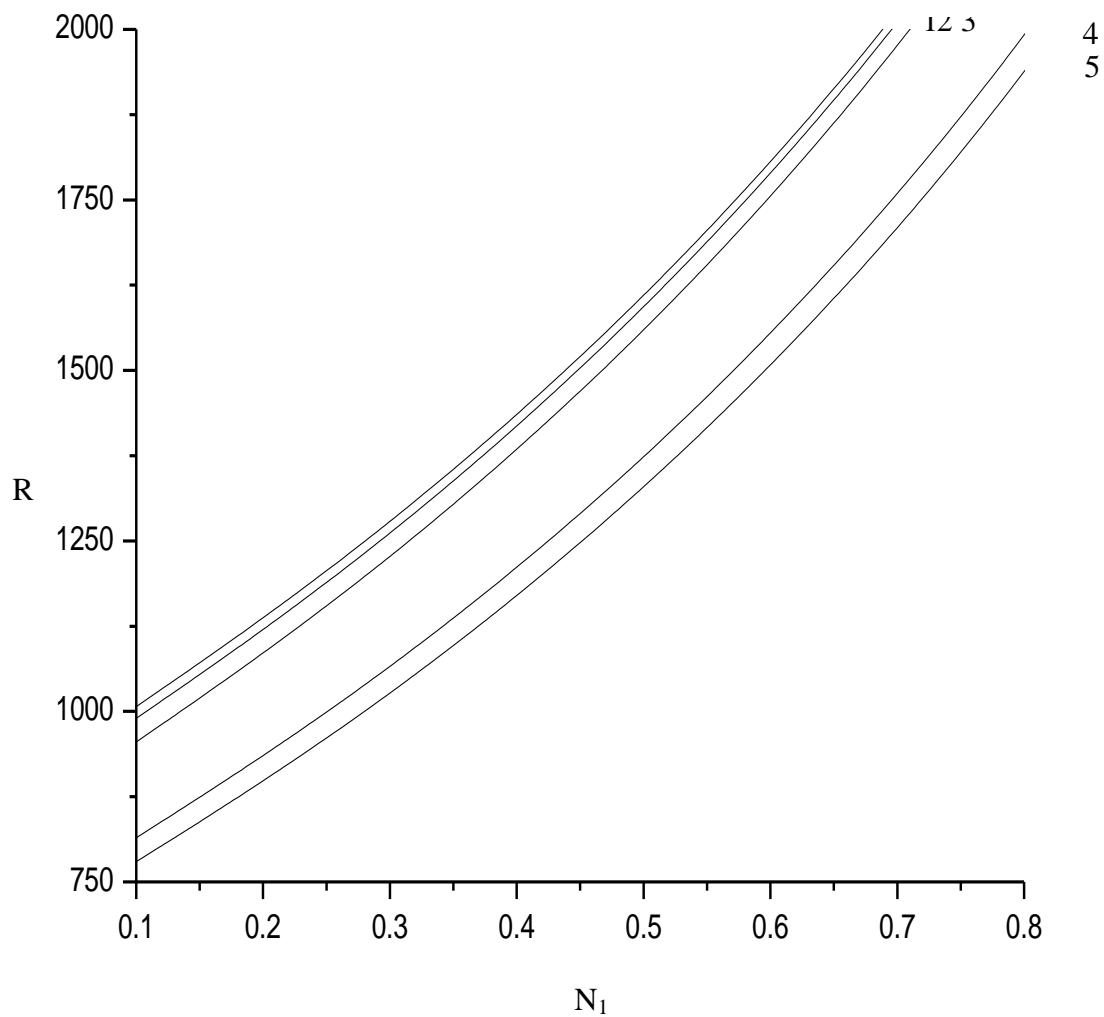


Figure 2: Plot of critical Rayleigh number R versus coupling parameter N_1 for different values of electric Rayleigh number L and ratio of diffusivity Γ .

1 $L = 50, \Gamma = 0.1, N_1 = 0.1, N_5 = 1, R_s = 25$

2 $L = 100, \Gamma = 0.1, N_1 = 0.1, N_5 = 1, R_s = 25$

3 $L = 200, \Gamma = 0.1, N_1 = 0.1, N_5 = 1, R_s = 25$

4 $L = 100, \Gamma = 0.3, N_1 = 0.1, N_5 = 1, R_s = 25$

5 $L = 100, \Gamma = 0.5, N_1 = 0.1, N_5 = 1, R_s = 25$

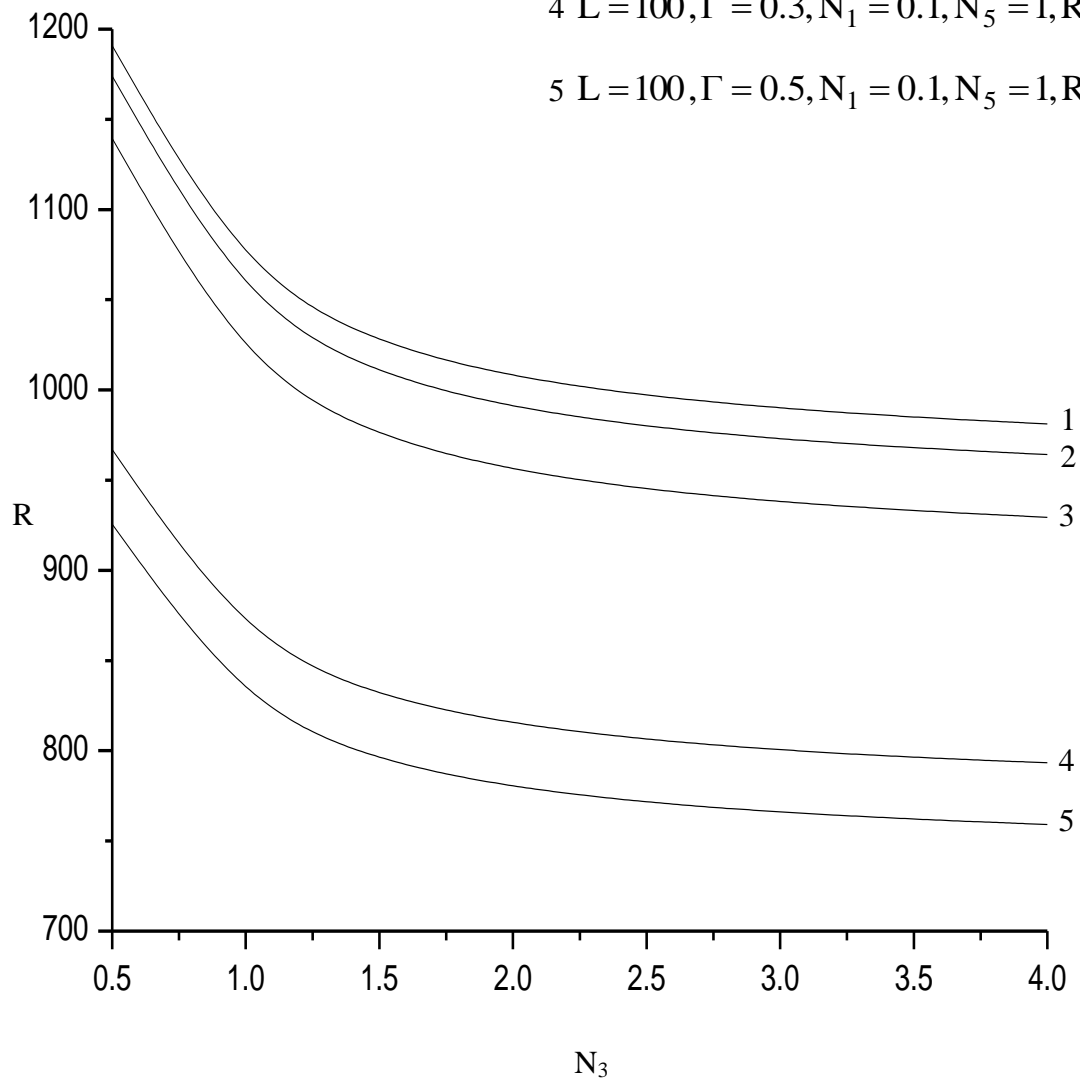


Figure 3: Plot of critical Rayleigh number R versus couple stress parameter N_3 for different values of electric Rayleigh number L and ratio of diffusivity Γ .

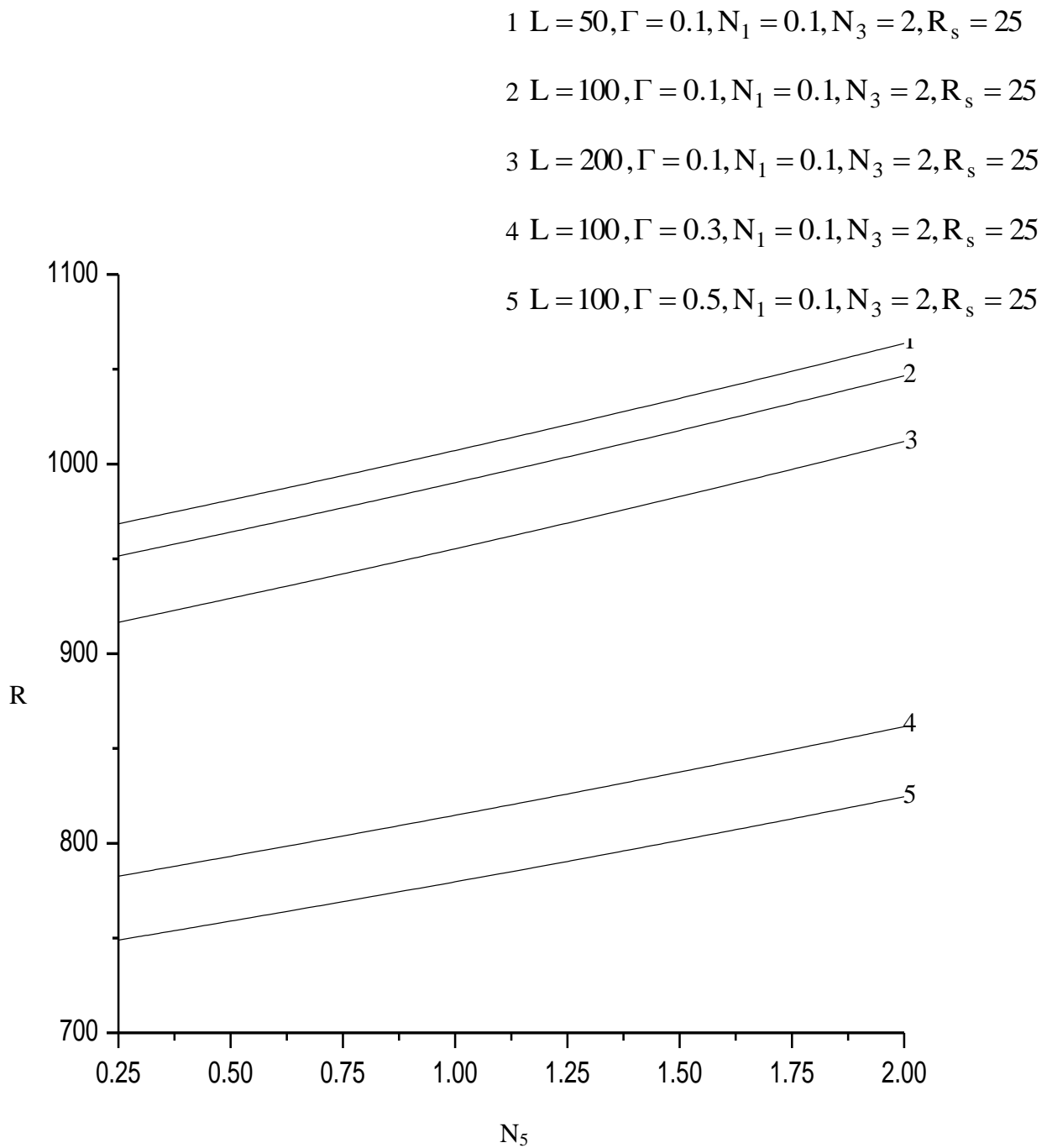


Figure 4: Plot of critical Rayleigh number R versus micropolar heat conduction parameter N_5 for different values of electric Rayleigh number L and ratio of diffusivity Γ .

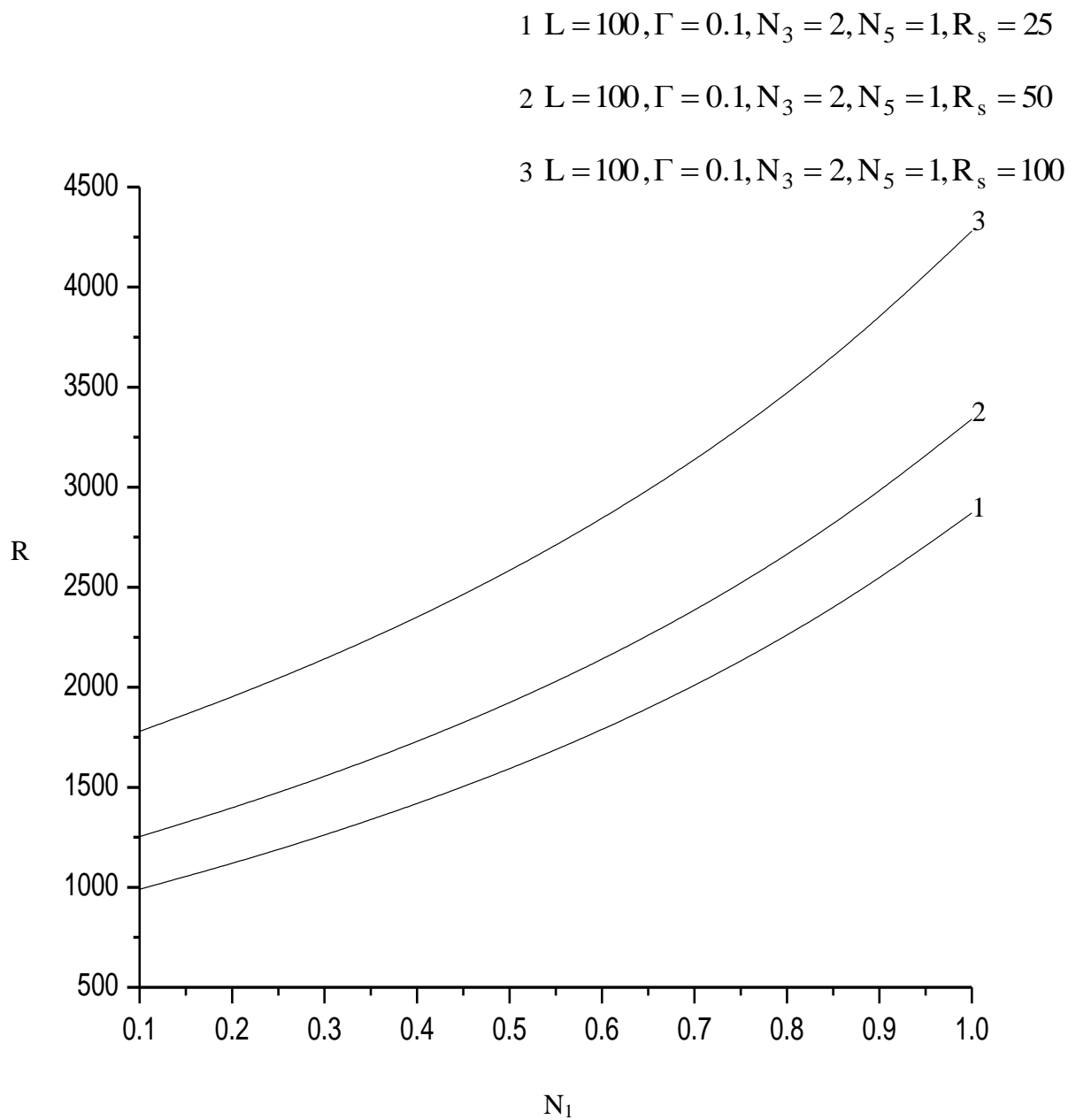


Figure 5: Plot of critical Rayleigh number R versus coupling parameter N_1 for different values of solutal Rayleigh number R_s .

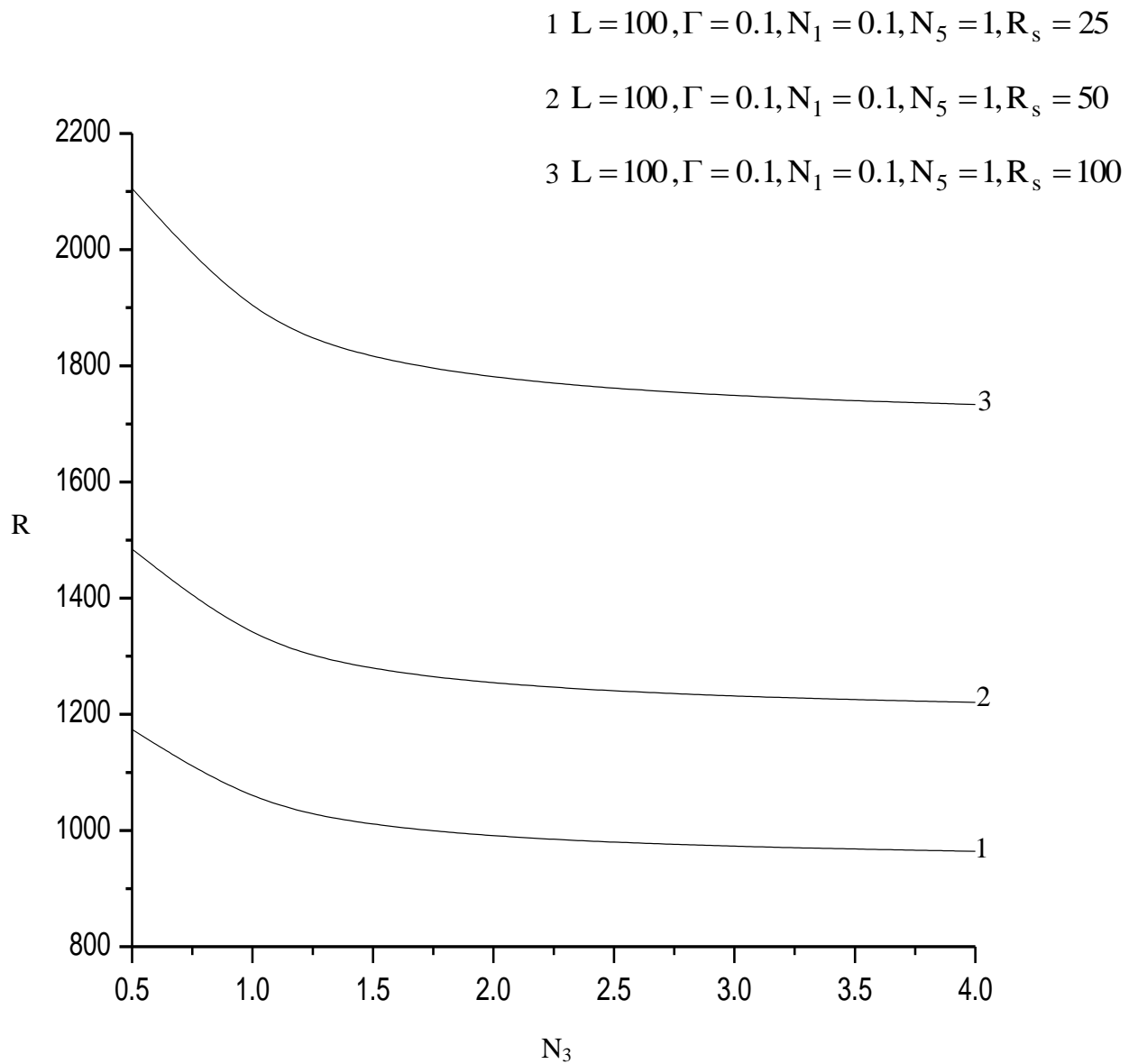


Figure 6: Plot of critical Rayleigh number R versus couple stress parameter N_3 for different values of solutal Rayleigh number R_s .

1 $L = 100, \Gamma = 0.1, N_1 = 0.1, N_3 = 2, R_s = 25$

2 $L = 100, \Gamma = 0.1, N_1 = 0.1, N_3 = 2, R_s = 50$

3 $L = 100, \Gamma = 0.1, N_1 = 0.1, N_3 = 2, R_s = 100$

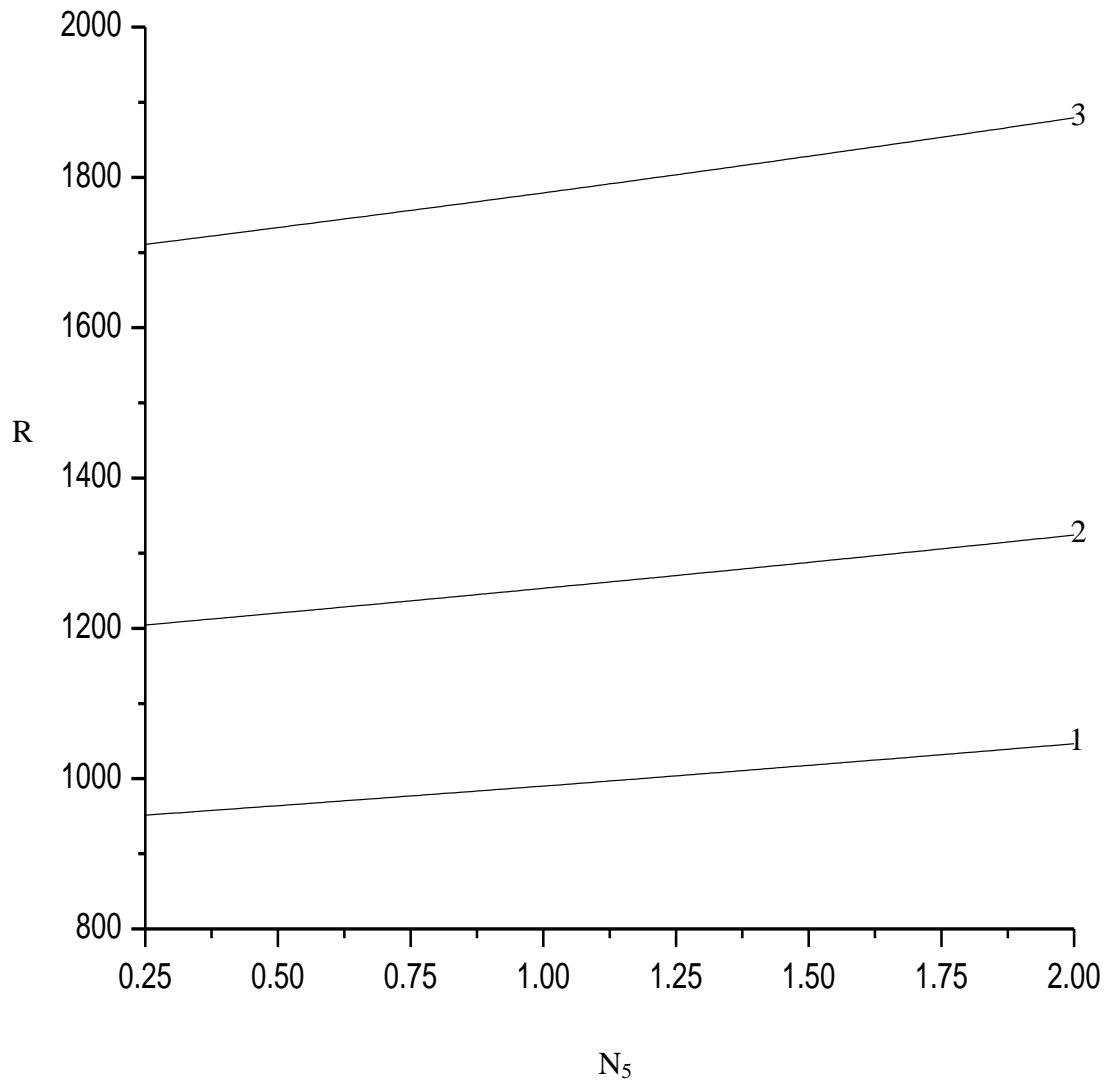


Figure 7: Plot of critical Rayleigh number R versus micropolar heat conduction parameter N₅ for different values of solutal Rayleigh number R_s.

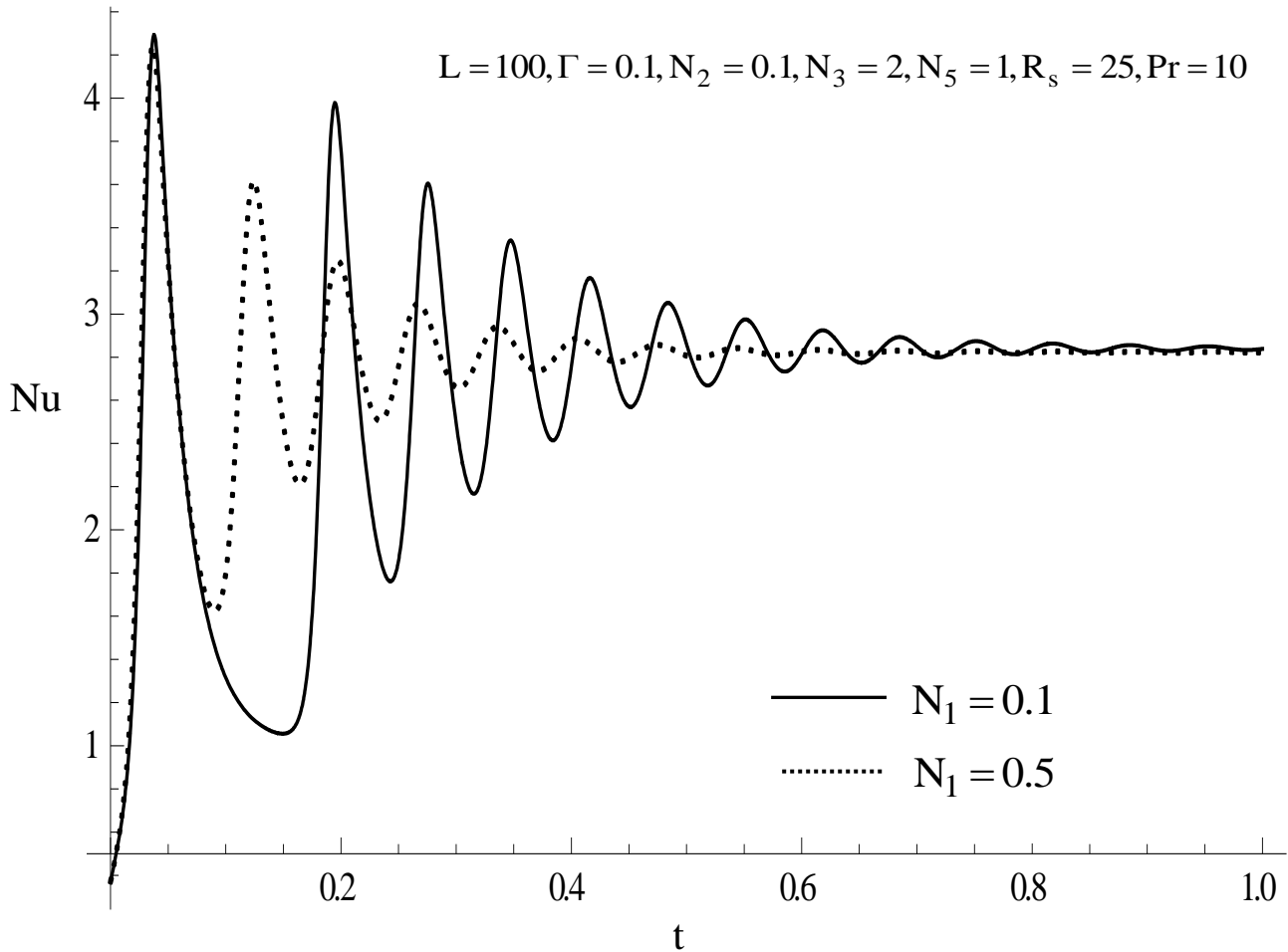


Figure 8: Plot of Nusselt number Nu versus time t for different values of coupling parameter N_1 .

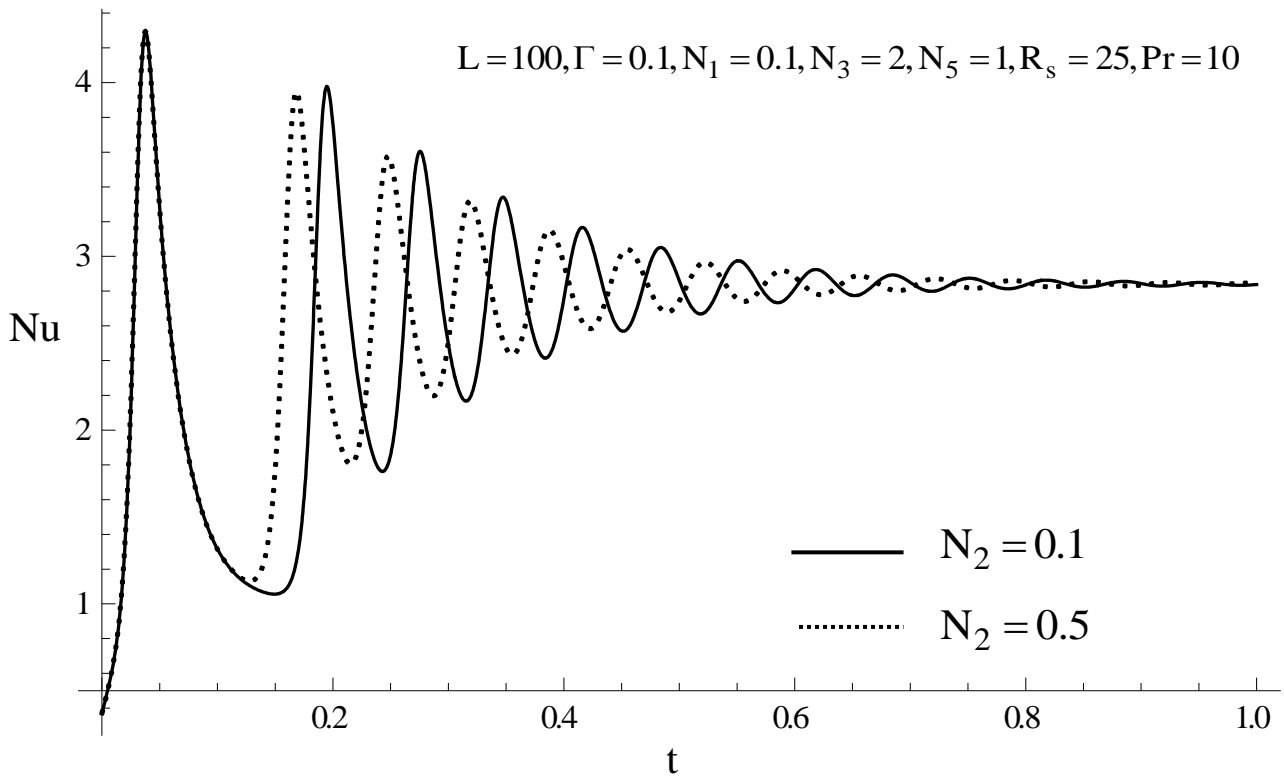


Figure 9: Plot of Nusselt number Nu versus time t for different values of inertia parameter N_2 .

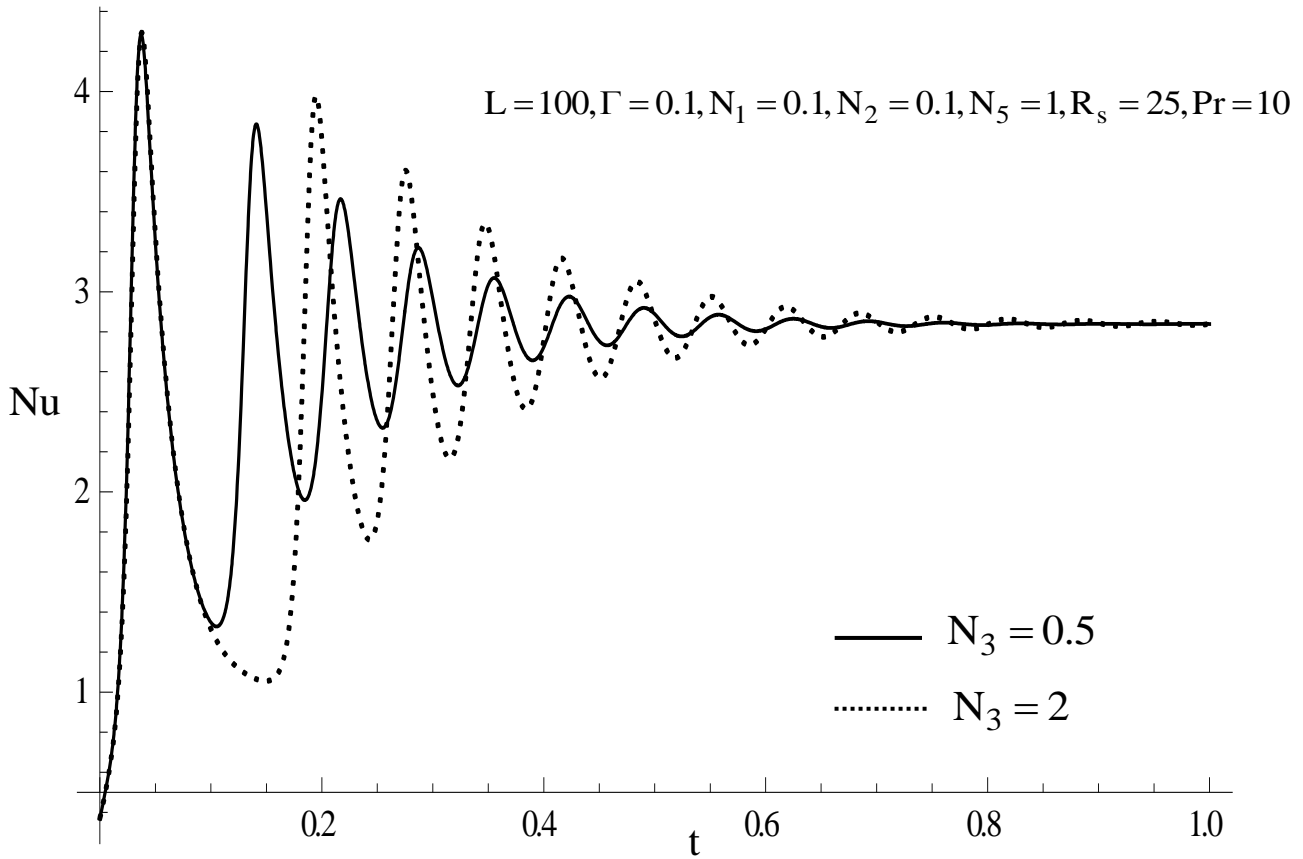


Figure 10: Plot of Nusselt number Nu versus time t for different values of couple stress parameter N_3 .

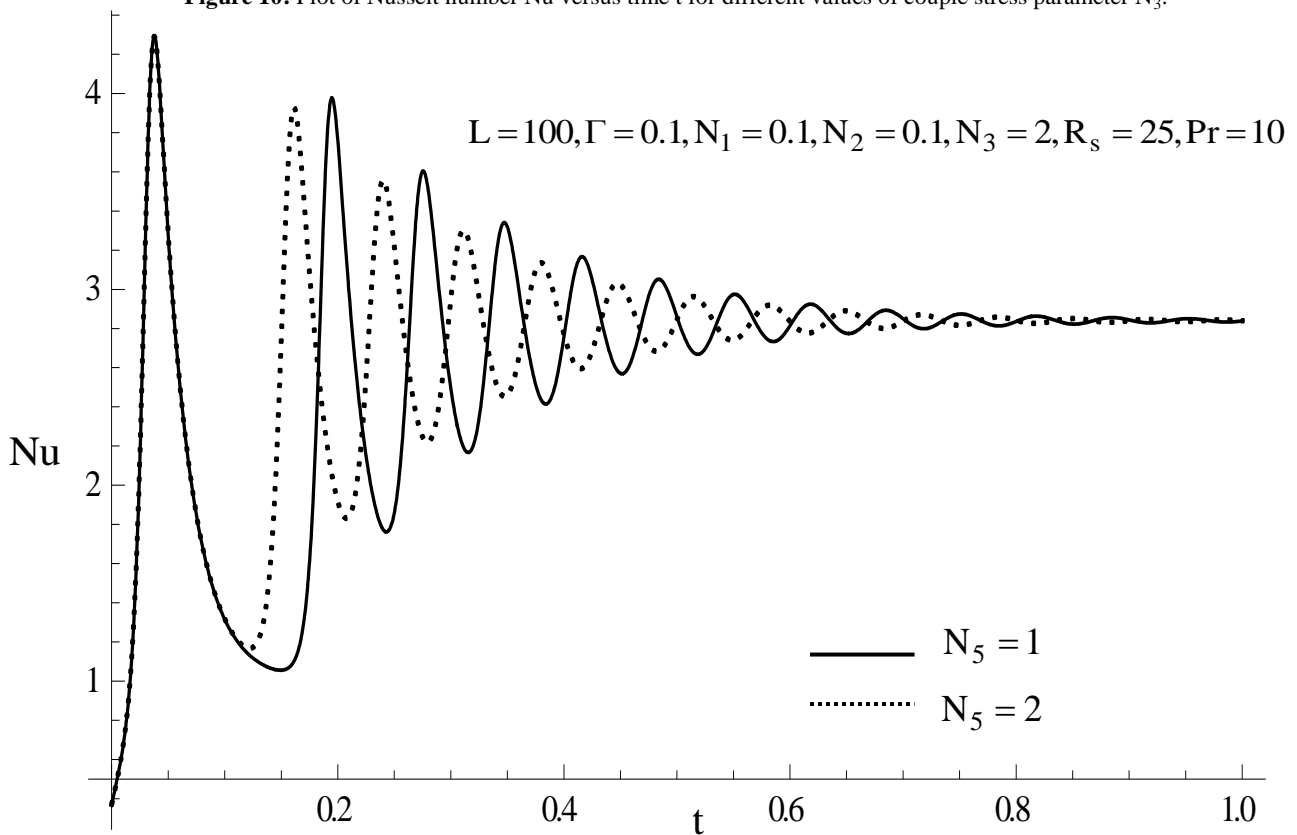


Figure 11: Plot of Nusselt number Nu versus time t for different values of micropolar heat conduction parameter N_5 .

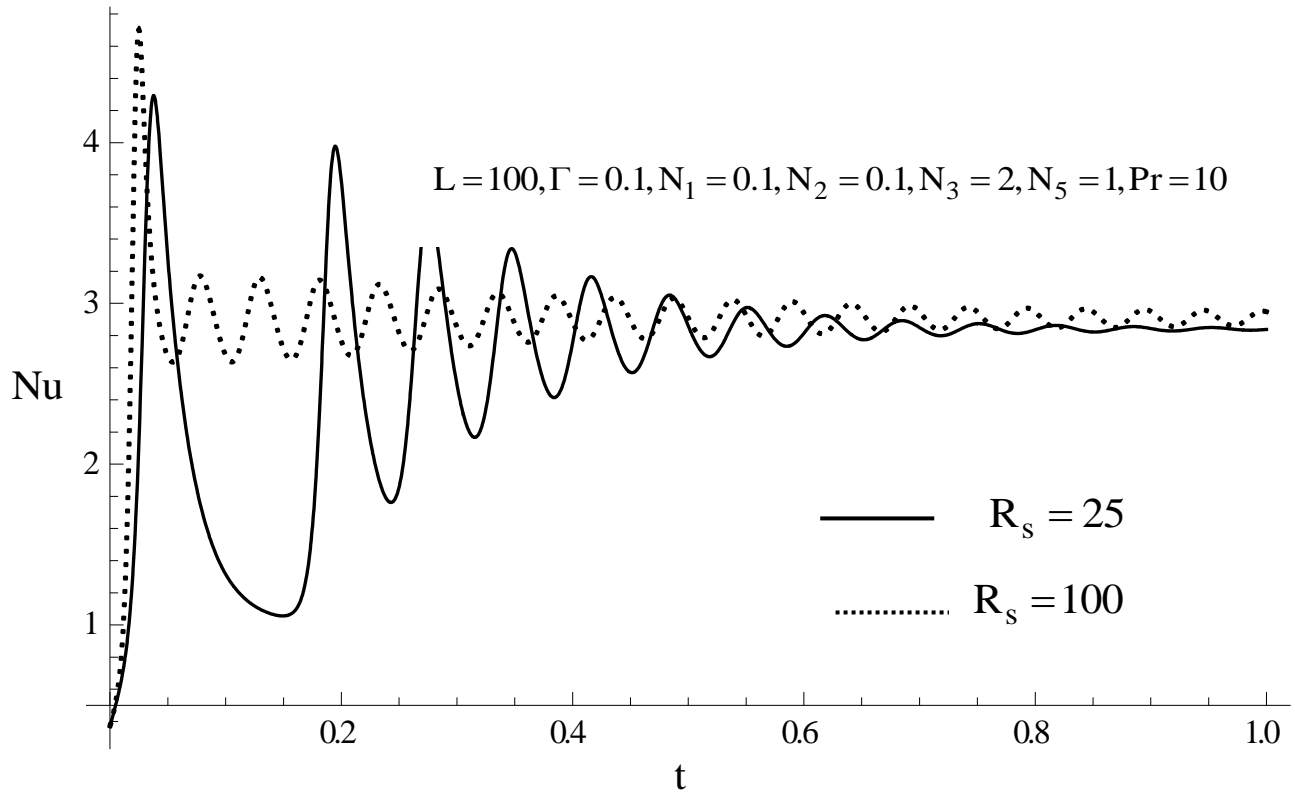


Figure 12: Plot of Nusselt number Nu versus time t for different values of solutal Rayleigh number R_s .

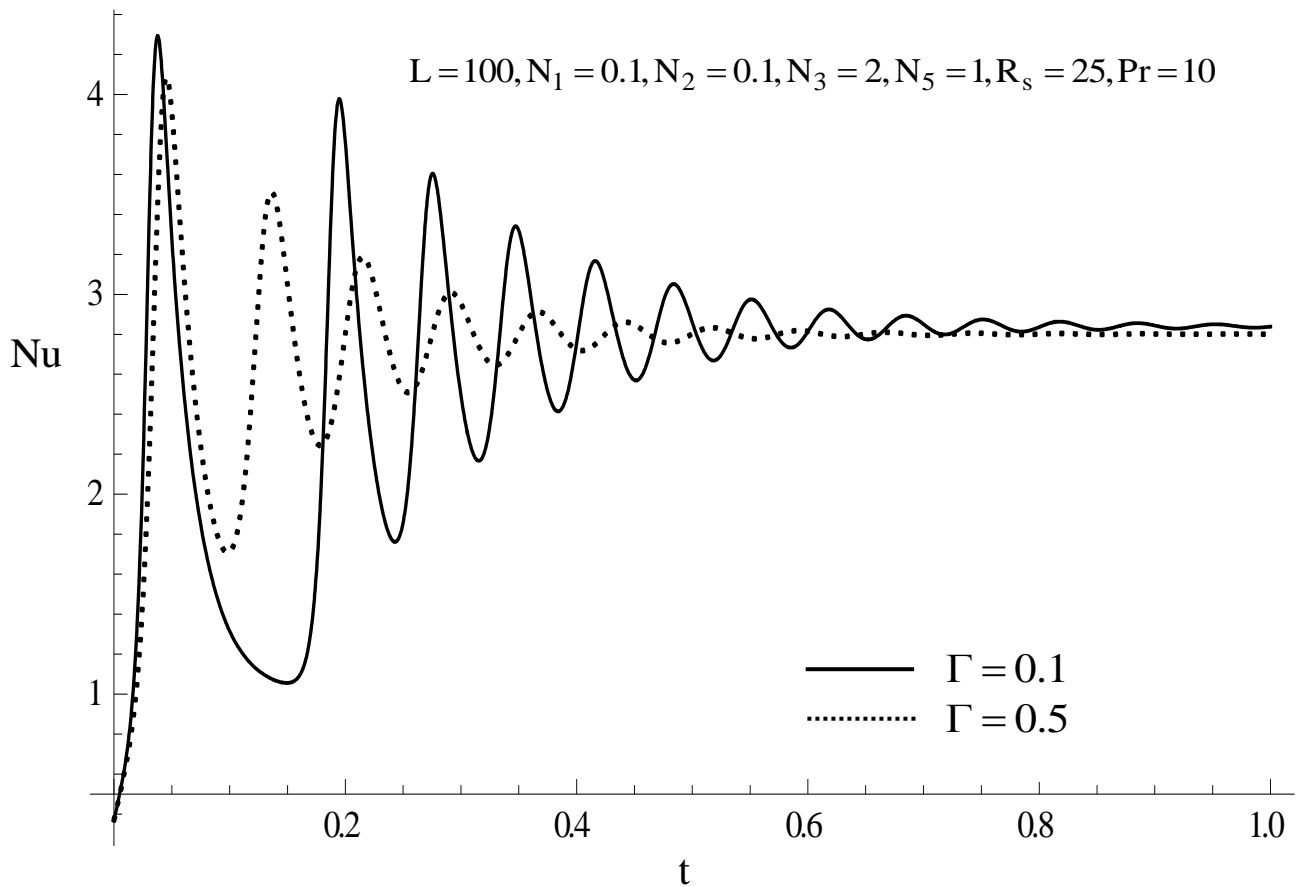


Figure 13: Plot of Nusselt number Nu versus time t for different values of ratio of diffusivity Γ .

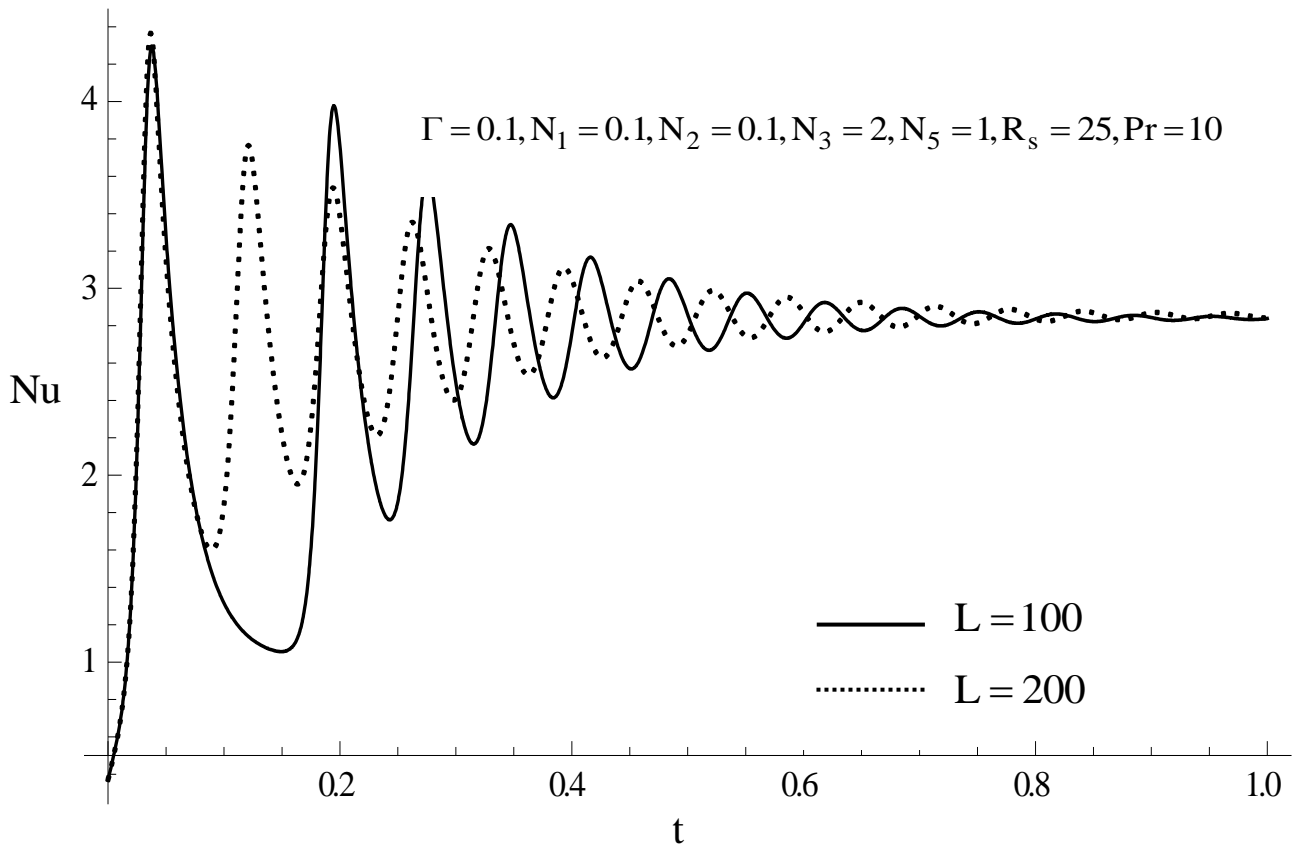


Figure 14: Plot of Nusselt number Nu versus time t for different values of electric Rayleigh number L .

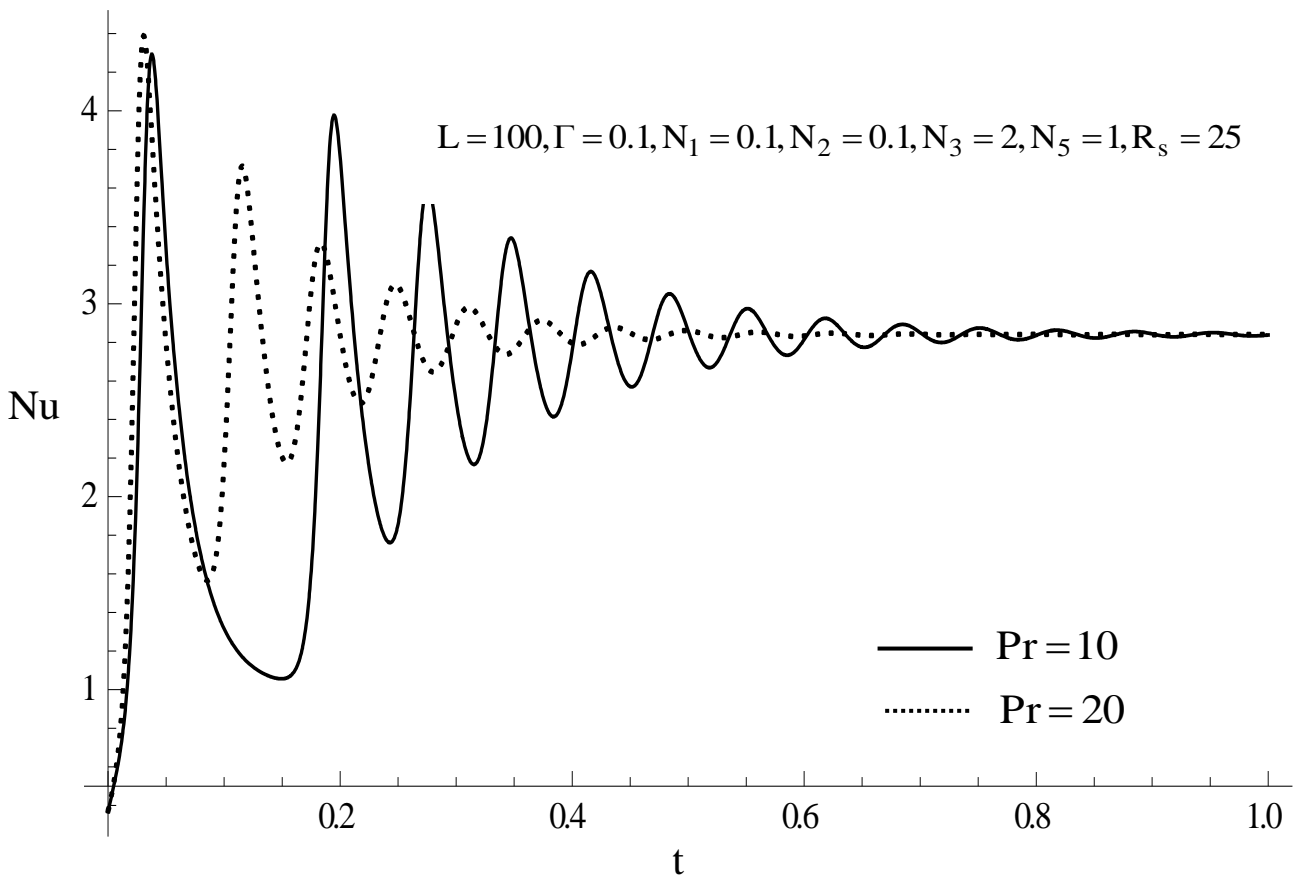


Figure 15: Plot of Nusselt number Nu versus time t for different values of Prandtl number Pr .

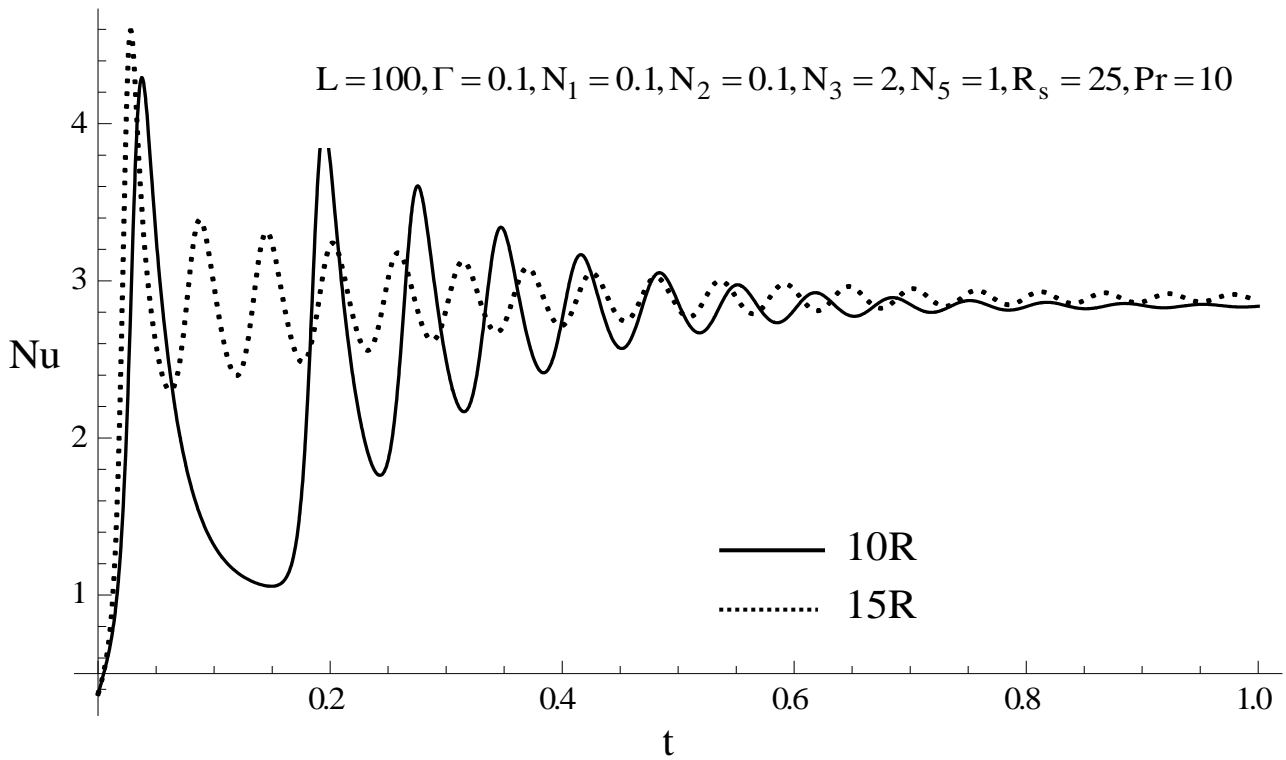


Figure 16: Plot of Nusselt number Nu versus time t for different values of critical Rayleigh number R.

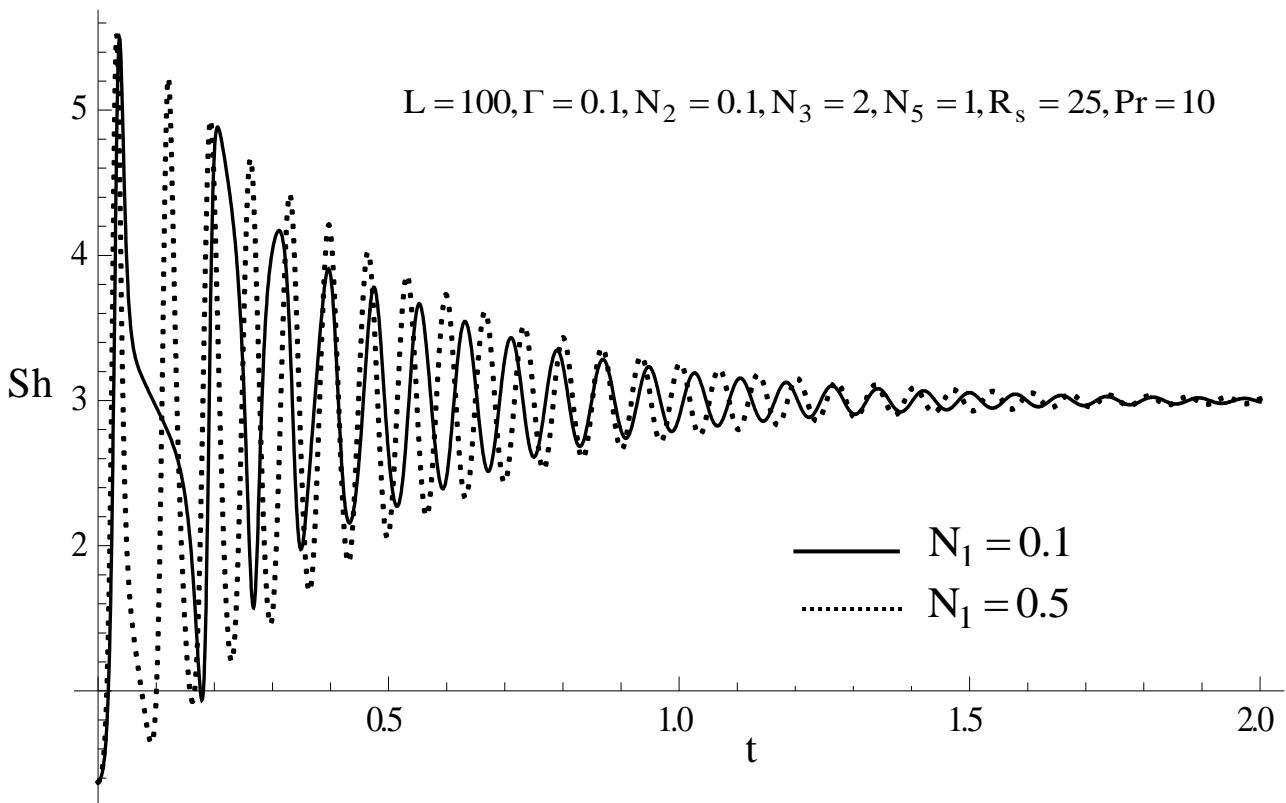


Figure 17: Plot of Sherwood number Sh versus time t for different values of coupling parameter N_1 .

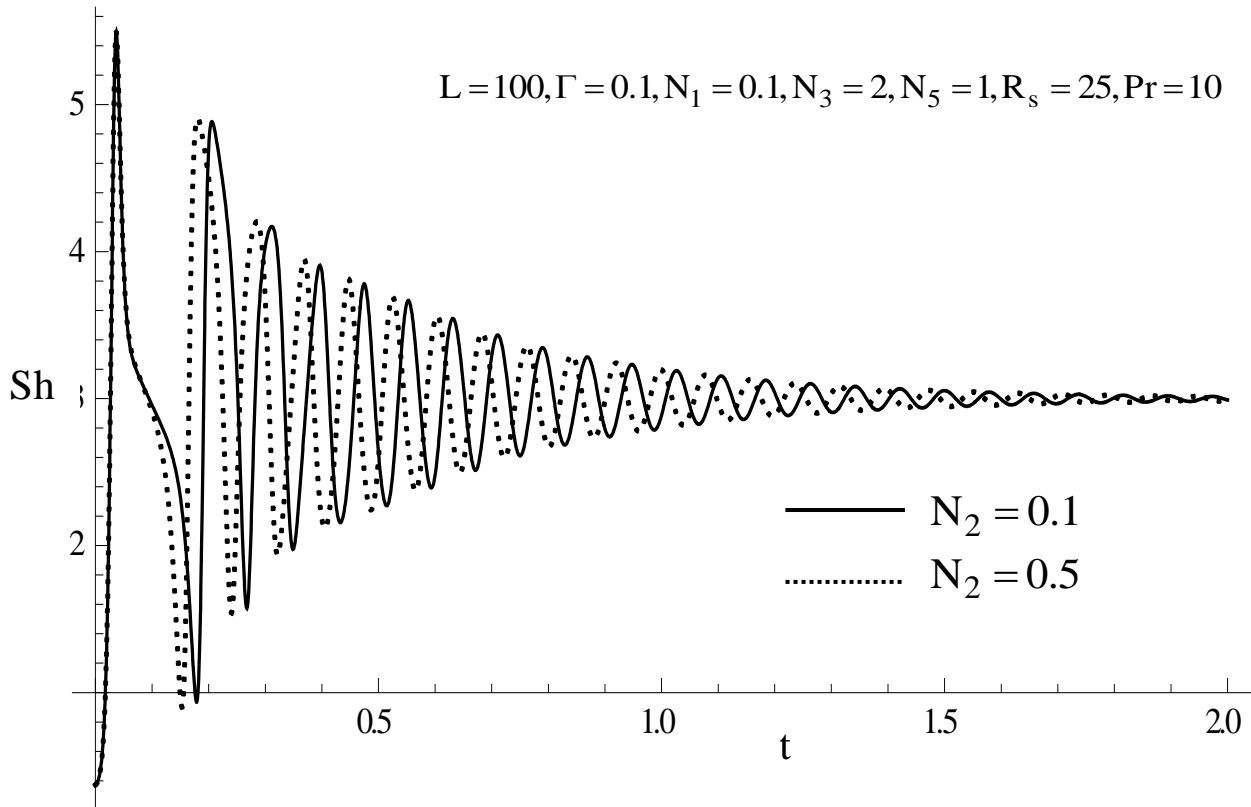


Figure 18: Plot of Sherwood number Sh versus time t for different values of inertia parameter N_2 .

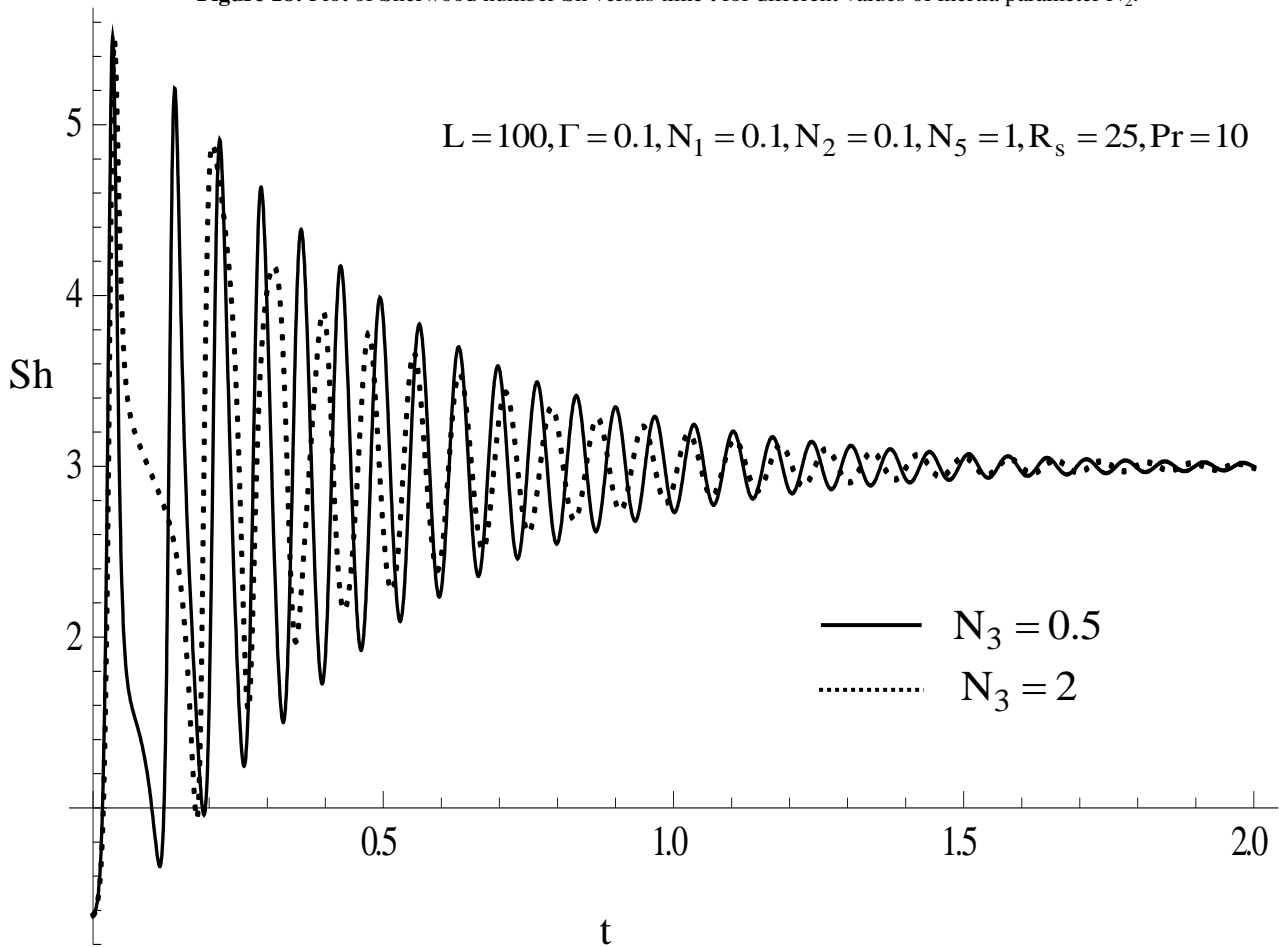


Figure 19: Plot of Sherwood number Sh versus time t for different values of couple stress parameter N_3 .

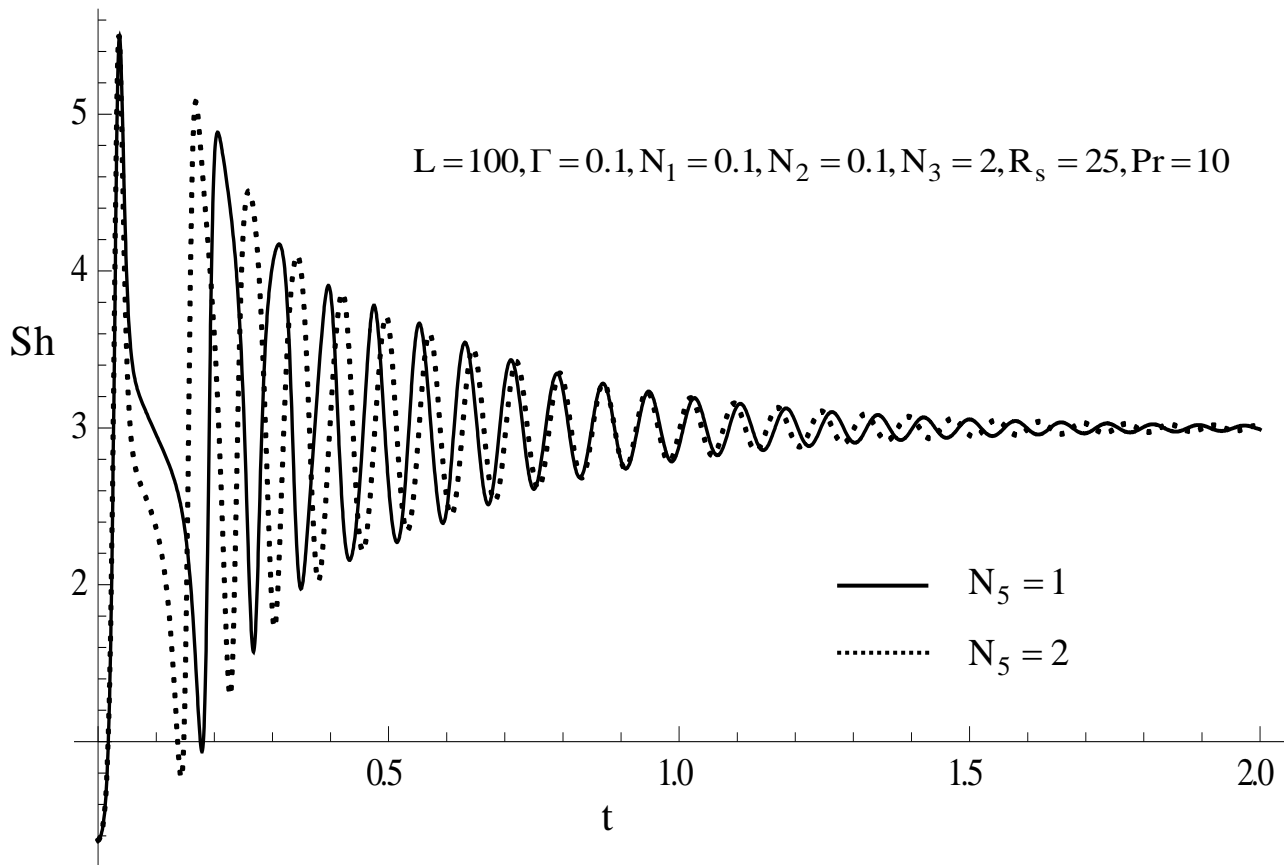


Figure 20: Plot of Sherwood number Sh versus time t for different values of micropolar heat conduction parameter N_5 .

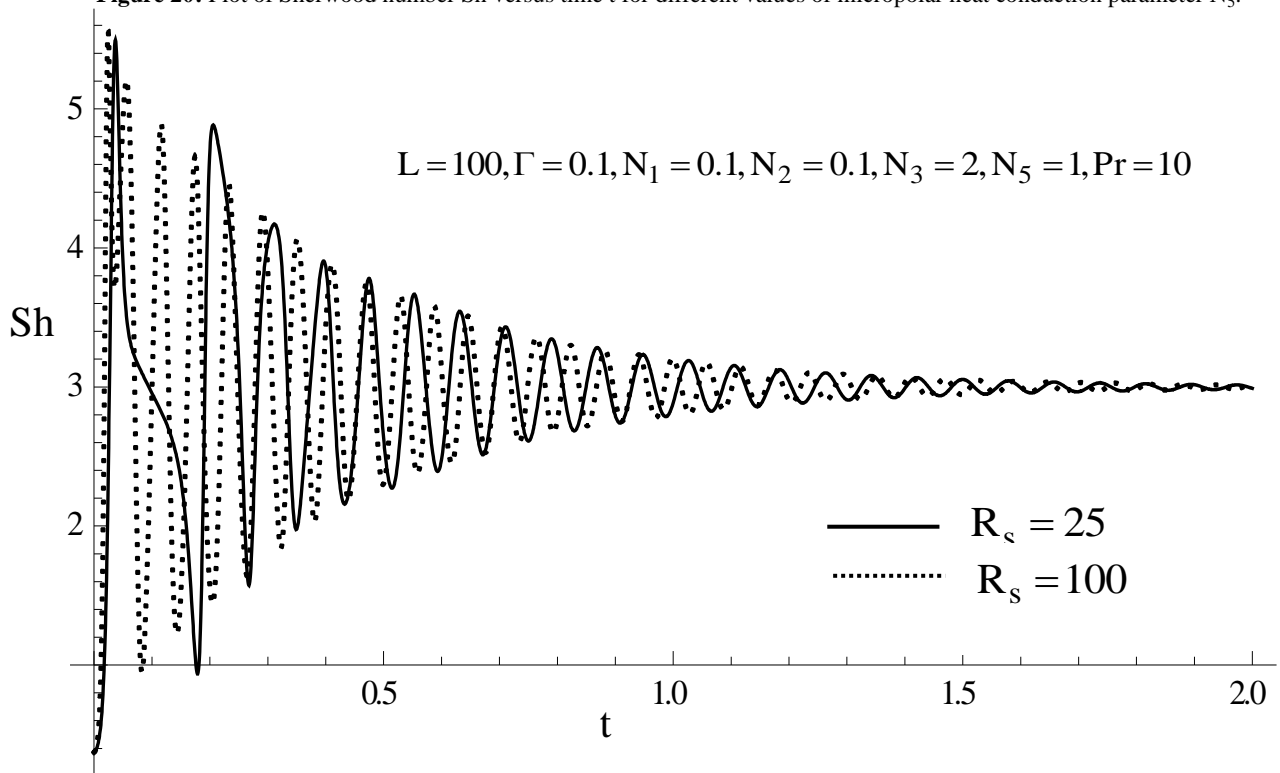


Figure 21: Plot of Sherwood number Sh versus time t for different values of solutal Rayleigh number R_s .

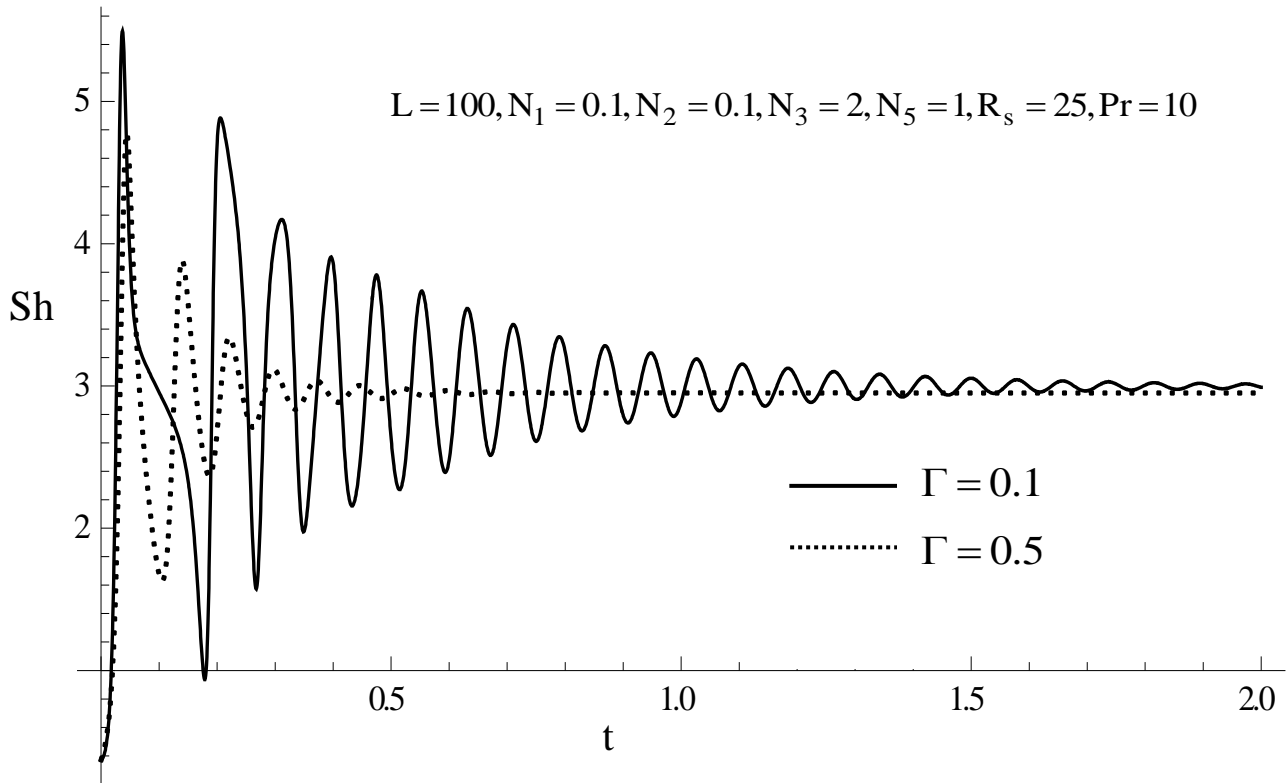


Figure 22: Plot of Sherwood number Sh versus time t for different values of ratio of diffusivity.

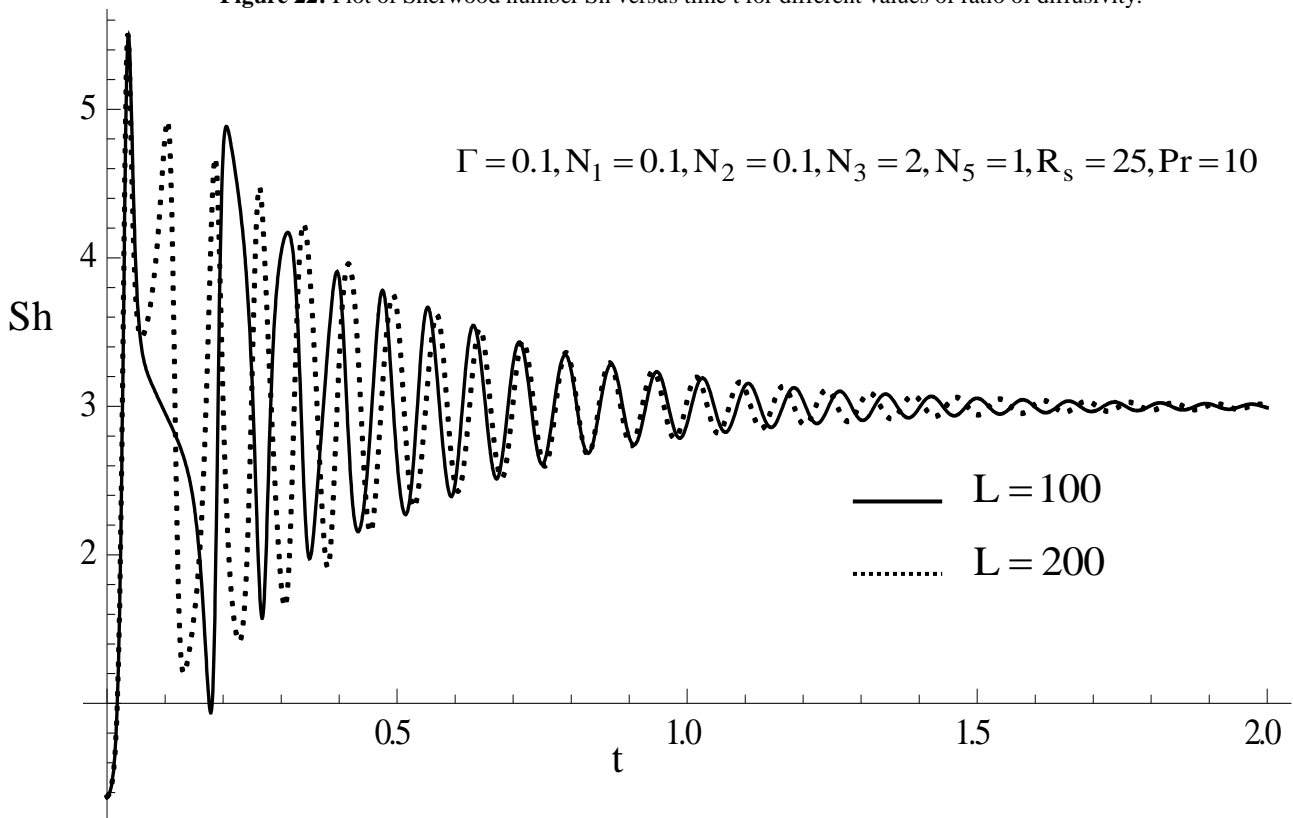


Figure 23: Plot of Sherwood number Sh versus time t for different values of electric Rayleigh number L .

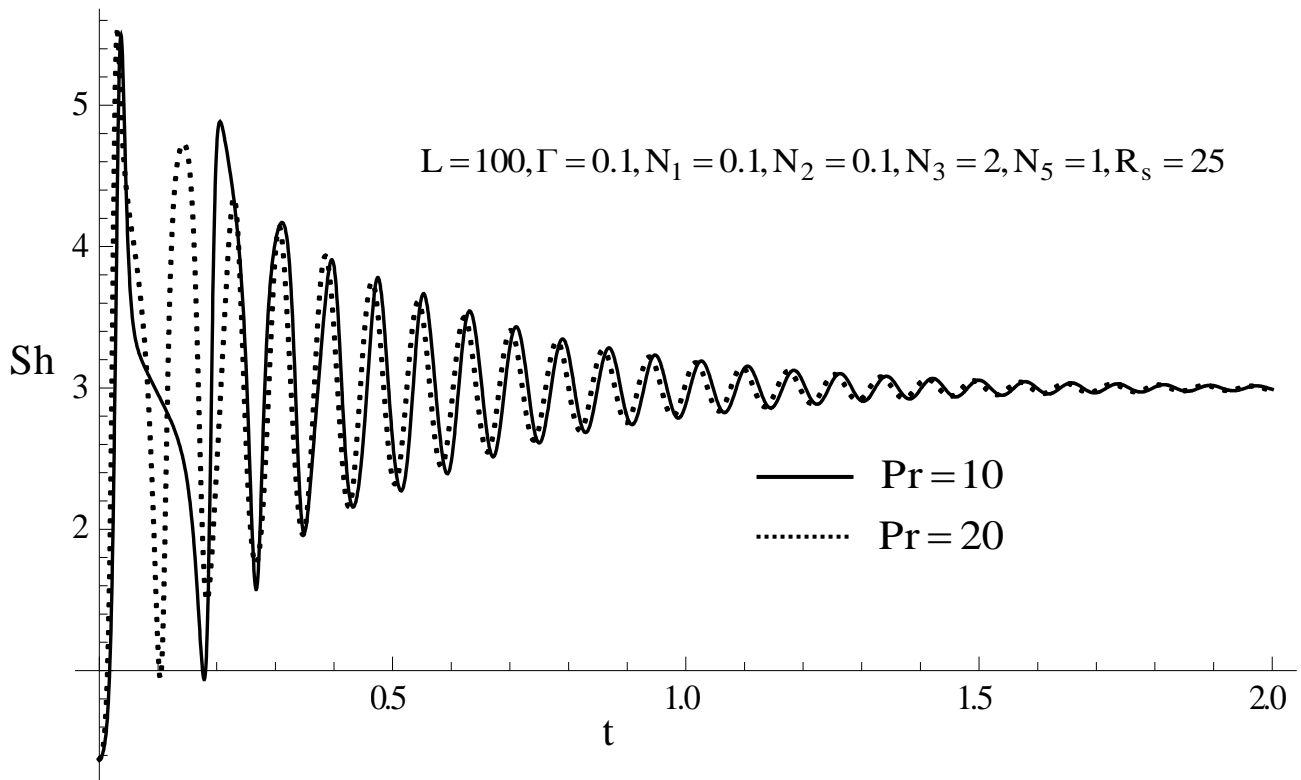


Figure 24: Plot of Sherwood number Sh versus time t for different values of Prandtl number Pr .

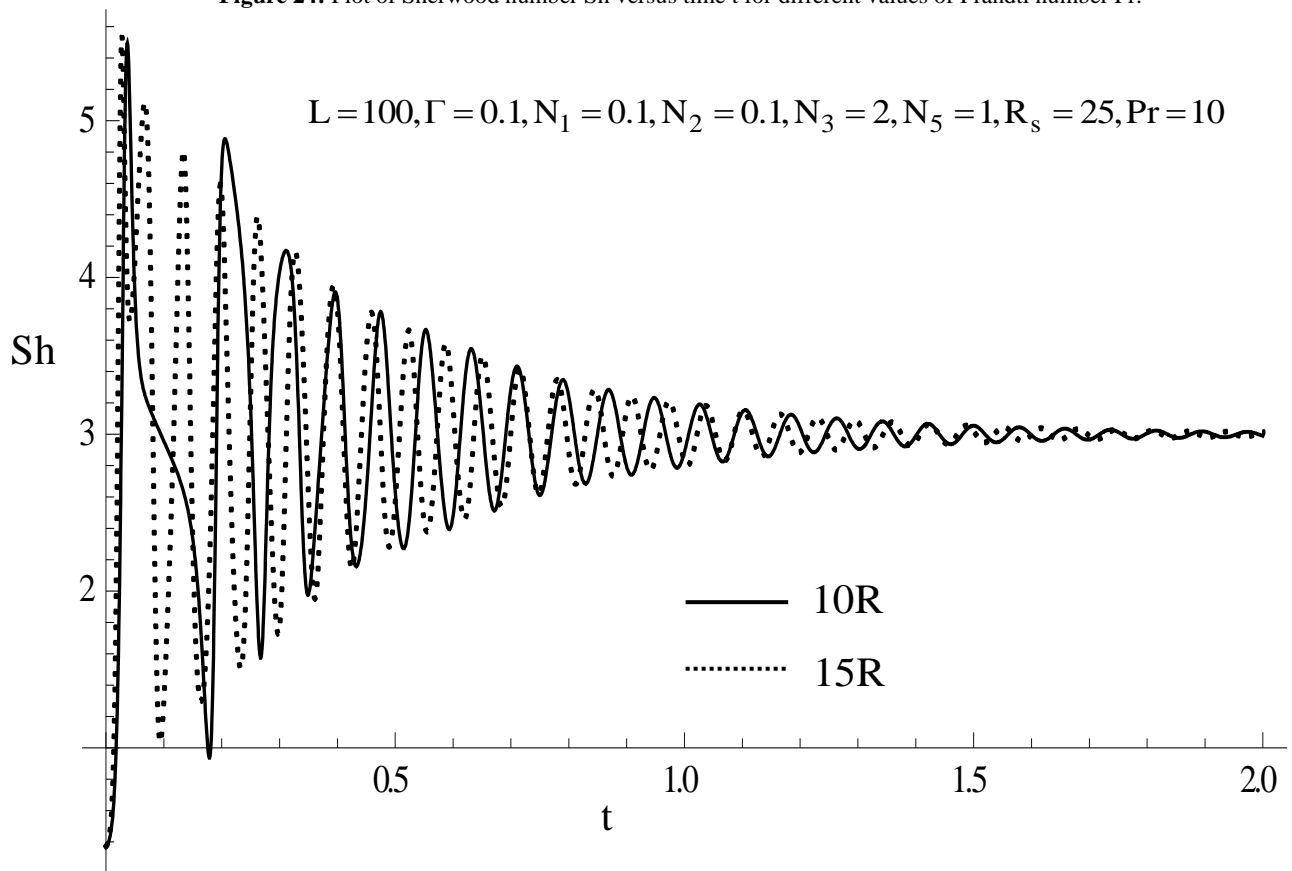


Figure 25: Plot of Sherwood number Sh versus time t for different values of critical Rayleigh number R .

In this section, we first discuss the linear theory followed by a discussion of non-linear theory.

Figure (2) is the plot of critical Rayleigh number R_c versus coupling parameter N_1 for different values of electric Rayleigh number L . It is observed that as N_1 increases, R_c also increases. Thus, increase in the concentration of suspended particles stabilizes the system. Figure (3) is the plot of R_c versus couple stress parameter N_3 for different values of L . We note that the role played by the shear stress in the conservation of linear momentum is played by the couple stress in angular momentum equations. It is observed that, increase in N_3 decreases R_c . From the figure, we see that the effect of N_3 on the system is very small compared to the effects of the other micropolar parameters characterising the suspended particles. Figure (4) is the plot of R_c versus micropolar heat conduction parameter N_5 for different values of L . From the figure it is clear that when the coupling between temperature and spin increases the system is more stable compared to the case when there is no coupling. The reason for the observed effects of N_1 , N_3 and N_5 on convection is explained in table (1). From the above figures we also observe that, increase in L decreases R_c . The electric Rayleigh number L is the ratio of electric force to the dissipative force. For higher values of L the dissipative force becomes negligible and hence it destabilizes the system.

Figure (5), (6) and (7) are the plots of R_c versus N_1 , N_3 and N_5 for different values of solutal Rayleigh number R_s and ratio of diffusivity Γ . It is observed that, increase in R_s increases R_c , indicating that the effect of R_s is to inhibit the onset of convection. Positive values of R_s are considered and in such a case, one gets positive values of R and these signify the assumption of a situation in which we have cool fresh water overlying warm salty water. In the absence of cross diffusion, this situation is conducive for the appearance of salt fingers which arises in a stationary regime of onset of convection. From the figure it is also observed that increasing the value of Γ decreases the R_c , indicating that Γ destabilizes the system. This is because when $\Gamma > 1$ the diffusivity of heat is more than the diffusivity of solute and therefore, solute gradient augments the onset of convection.

We now discuss the influence of micropolar parameters, solutal Rayleigh number, ratio of diffusivity, electric Rayleigh number, Prandtl number and critical Rayleigh number on the onset of double diffusive convection and also the role of heat and mass transfer in the non-linear system.

In the study of convection, the determination of heat and mass transport across the layer plays a vital role which are quantified in terms of Nusselt number (Nu) and Sherwood number (Sh).

From the figures of Nusselt number Nu, it is observed that the curve Nu versus time t starts with $Nu = 1$, signifying the initial conduction state. As time progresses, the value of Nu increases, thus showing that convective regime is in place and then finally the curve of Nu level off at long times. It is also observed that for shorter times the nature of Nu is oscillatory.

Figures (8) – (11) are the plots of Nu versus t for different values of N_1 , N_2 , N_3 and N_5 respectively. From the figures it is observed that increase in N_1 and N_5 reduces the heat transfer. This is because in the presence of suspended particles the critical Rayleigh number increases and hence the Nusselt number decreases. It is also found that increase in N_2 , N_3 increases the heat transfer. This is because the inertia parameter and the couple stress parameter decrease the critical Rayleigh number and hence increase the Nusselt number.

Figures (12) – (15) are the plots of Nu versus t for different values of R_s , Γ , L and Pr respectively. It is observed from the figures that increase in these parameters decreases the heat transfer. Figure (16) is a plot of Nu vs t for different values of Rayleigh number. It is observed that when the Rayleigh number is increased ten times and fifteen times, the rate of heat transfer is not uniform in the beginning and as time increases the rate of heat transfer reaches a steady state and is uniform. Also it is observed that Nu is fluctuating throughout the system as a result the rate of heat transfer is less. For a slight change in the initial condition the same situation can be observed in figure (16) in which Nu is fluctuating more often throughout the system when Rayleigh number is increased to ten times as well fifteen times. This shows that chaos sets for higher value of Rayleigh number and chaos are very sensitive to the initial condition, hence difficult to measure the rate of heat transfer in the system. It is also clear from the figures (12) – (15) that the phase space of the system is not uniform.

The figures (17) – (25) depicts the fact that Sherwood number variations with N_1 , N_2 , N_3 , N_5 , R_s , Γ , L , Pr and R are similar to what was seen with Nu in figures (8) – (16) but the effects are reversed.

IX. Conclusions

The effect of coupling parameter N_1 , micropolar heat conduction parameter N_5 , electric Rayleigh number L and solutal Rayleigh number R_s is to reduce the amount of heat transfer and increase the mass transfer, whereas the opposite effect is observed in the case of inertia parameter N_2 and the couple stress parameter N_3 . Thus it is possible to control the onset of double diffusive convection and also regulate the heat and mass transfer with the help of micropolar fluid and electric field.

Acknowledgement

The authors would like to acknowledge management of Christ University for their support in completing the work.

Bibliography

- [1]. Ahmadi G (1976). Stability of micropolar fluid layer heated from below. International Journal of Engineering Science14, pp. 81-85.
- [2]. Bhadauria BS and Palle Kiran (2014). Weak nonlinear double-diffusive magnetoconvection in a newtonian liquid under temperature modulation. International Journal of Engineering Mathematics, pp. 1-11.
- [3]. Bhattacharya SP and Jena SK (1983). On the stability of hot layer of micropolar fluid. International Journal of Engineering Science21(9), pp. 1019-1024.
- [4]. Chandrasekhar S (1961). Hydrodynamic and hydromagnetic stability. Oxford: Clarendon Press.
- [5]. Datta AB and Sastry VUK (1976). Thermal instability of a horizontal layer of micropolar fluid heated from below. International Journal of Engineering Science14(7), pp. 631-637.

- [6]. Eringen AC (1964). Simple microfluids. *International Journal of Engineering Science*2(2), pp. 205-217.
- [7]. Eringen AC (1966). A unified theory of thermomechanical materials. *International Journal of Engineering Science*4(2), pp. 179-202.
- [8]. Eringen AC (1972). Theory of thermomicrofluids. *Journal of Mathematical Analysis and Applications*38(2), pp. 480-496.
- [9]. Jin YY and Chen CF (1997). Effect of gravity modulation on natural convection in a vertical slot. *International Journal of Heat and Mass Transfer* 40(6), pp. 1411-1426.
- [10]. Joseph TV et al. (2013). Effect of non-uniform basic temperature gradient on the onset of Rayleigh-Bénard-Marangoni electro-convection in a micropolar fluid. *Applied Mathematics* 4(8), pp. 1180-1188.
- [11]. Lebon G and Perez-Garcia C (1981). Convective instability of a micropolar fluid layer by the method of energy. *International Journal of Engineering Science*19(10), pp. 1321-1329.
- [12]. Lukaszewicz G (1999). *Micropolar fluid theory and applications*. Boston: Birkhauser.
- [13]. Malashetty MS et al. (2006). An analytical study of linear and non-linear double diffusive convection with Soret effects in couple stress liquids. *International Journal of Thermal Science* 45, pp. 897-907.
- [14]. Melvin E Stern (1960). The "Salt-Fountain" and Thermohaline Convection. *Tellus* 12(2), pp. 172-175.
- [15]. Power H (1995). *Bio-Fluid Mechanics: Advances in Fluid Mechanics*, U.K.: W.I.T. Press.
- [16]. Pranesh S and Arun Kumar N (2012).Effect of non-uniform basic concentration gradient on the onset of double-diffusive convection in micropolar fluid.*Applied Mathematics*3, pp. 417-424.
- [17]. Pranesh S and Riya Baby (2012).Effect of non-uniform temperature gradient on the onset of Rayleigh-Bénardelectroconvection in a micropolar fluid.*Applied Mathematics*3, pp. 442-450.
- [18]. Pranesh S et al. (2014).Linear and Weakly Non-Linear Analyses of Gravity Modulation and Electric Field on the onset of Rayleigh-Bénard Convection in a Micropolar Fluid. *Journal of Advances in Mathematics* 9(3), pp. 2057-2082.
- [19]. Rama Rao KV (1980). Thermal instability in a micropolar fluid layer subject to a magnetic field. *International Journal of Engineering Science*18(5), pp. 741-750.
- [20]. Siddheshwar PG and Pranesh S (1998) Effect of a non-uniform basic temperature gradient on Rayleigh-Bénard convection in a micropolar fluid. *International Journal of Engineering Science*36(11), pp. 1183-1196.
- [21]. Turner JS (1973).*Buoyancy effects in fluids*. Cambridge University Press.
- [22]. Veronis G (1959). Cellular convection with finite amplitude in a rotating fluid.*Journal of fluid mechanics* 5, pp. 401-435.